Effect of the Chemical Treatment on the Inorganic Content of Kenaf Fibers and on the Performance of Kenaf-Polypropylene Composites

by

Nikole Lyn

A thesis
presented to the University of Waterloo
in fulfillment of the
thesis requirement for the degree of
Master of Applied Science
in
Chemical Engineering

Waterloo, Ontario, Canada, 2018

Author's Declaration

I hereby declare that I am the sole author of this thesis. This is a true copy of the thesis, including any required final revisions, as accepted by my examiners.

I understand that my thesis may be made electronically available to the public.

…….

Abstract

Composites consisting of natural fibers and a polymer-based matrix have received considerable attention as an alternative to traditional mineral fibers such as glass-fiber. Composites containing natural fibers have the benefit of being light-weight and environmentally friendly but fall short with their mechanical properties, moisture resistance and thermal resistance, limiting their use to non-structural applications and low moisture environments.

The objective of this thesis was to evaluate kenaf fibers as an alternative natural fiber in the development of polypropylene composites. The chemical composition and inorganic content of kenaf fibers was quantified. The effect of alkalization of milled kenaf fiber (MKF) with sodium hydroxide on inorganic content was assessed. The effects of MKF alkalization and the addition of the coupling agent maleic anhydride were investigated.

MKF was treated for two hours with aqueous sodium hydroxide (NaOH) at different concentrations (0%, 3%, and 6%) and two temperatures (room temperature and 80°C). The treated MKF was analyzed by optical microscopy, scanning electron microscopy (SEM), thermogravimetric analysis (TGA), and chemical composition analysis to assess the effect of sodium hydroxide treatment. Optical microscopy showed the presence of thin protrusions with MKF treated with 3% and 6% NaOH at 80°C. SEM images showed a smoother fibrillar surface of MKF when treated with 3% and 6% NaOH at 80°C. TGA analysis indicated that the hemicellulose shoulder between 240°C and 325°C disappeared when treated with 3% and 6% NaOH at room temperature and 80°C indicating removal of hemicellulose. This was confirmed

by chemical composition analysis which showed a decrease in hemicellulose mass fraction and an increase in cellulose mass fraction when MKF was treated with NaOH at 3% and 6% at room temperature and 80°C.

The inorganic content for alkalized MKF was obtained with inductively coupled plasma optical emission spectroscopy (ICP) for 20 elements. Major elements (greater than 150 µg element/g fiber) were Fe, Ca, Na, Mg, K, Al, and B. Minor elements (less than 150 µg element/g fiber) were Ni, Mn, Ba, Zn, Pb, Sr, Cr, Y, Cu, Co, Cd, Li and V. Calcium had the greatest content (4503- 4982 µg element/g fiber). Analysis of variance (ANOVA) was used to determine the effects of NaOH treatment concentration and temperature on elemental concentration. Of the major elements, NaOH concentration had an effect on Fe, Ca, Na, K, Al and B while treatment temperature had an effect on Na, K and Al. The interaction between NaOH concentration and treatment temperature had an effect on all major elements. The inorganic elements analyzed by ICP accounted for 0.76-0.94 wt.% of kenaf depending on the alkali treatment conditions.

Composites were prepared with MKF subjected to alkalization treatments and polypropylene (PP) using twin-screw extrusion and injection molding. Polypropylene grafted maleic anhydride (MAPP) was added to assess its effect on composite performance. MKF-PP composites were tested for tensile strength (28.9-30.3 MPa), elongation at break (5.1-6.0%), and Young's Modulus (665.5-710.9 MPa). Tensile tests showed 3% and 6% NaOH treatment at room temperature and 80°C of MKF did not affect the mechanical performance (tensile strength, elongation at break, and Young's modulus) of the composite. Addition of MAPP to composites, with and without NaOH treatment, improved the tensile strength (31.6-35.0 MPa) of the composite. SEM showed that composites without MAPP had poor fiber wetting and showed

fiber pull out in the fractured composite cross-sections. SEM of MKF-PP composites with MAPP showed a polymer coating on the surface of MKF. Energy dispersive x-ray spectroscopy (EDX) analysis of composites showed carbon and oxygen on all composites. Room temperature treated MKF composites showed higher oxygen concentrations in samples without MAPP. 80°C treated MKF composites showed lower oxygen concentrations in samples without MAPP.

Future work should consider the effects of NaOH treatments at higher concentrations and temperature and their effects on cellulose, hemicellulose, lignin, and inorganic content. It would also be interesting to see if adding inorganic content to kenaf fiber alters its performance in polypropylene based composites.

Acknowledgements

Firstly, I would like to thank Dr. Christine Moresoli, my supervisor, for sharing her wisdom, giving advice when necessary and supporting me through this research process. Secondly, I would like to thank my lab mates Rasool Nasseri, Omar Mustafa Al-Kubaisi, Chu Yin Huang, Joseph Khouri, and Huayu Niu for their moral and scholastic support. I am thankful for the assistance from Rasool Nasseri and Ward Madill with thermogravimetric analysis. I am thankful to Omar Mustafa Al-Kubaisi for assistance in composite preparation.

I am also thankful to my readers Dr. Valerie Ward, and Dr. Tizazu Mekonnen for taking the time to review my thesis. I owe a special thanks to the Ontario Ministry of Agriculture, Food, and Rural Affairs for providing kenaf fibers used in this thesis. I would also like to thank my friends Krishna Iyer, Seville Scarcello and Ahmad Qureshi for their advice, support, and motivation throughout my education. Finally, I would like to thank my family for their ongoing support in my educational and professional pursuits.

Table of Contents

List of Figures

List of Tables

List of Abbreviations

ADF	acid detergent fiber
ANOVA	analysis of variance
ASTM	American Society for Testing and Materials
avg	average
DTG	differential thermogravimetric
EDS/EDX	energy dispersive X-ray spectroscopy
ha	hectare
HCl	hydrochloric acid
HF	hydrofluoric acid
HNO_3	nitric acid
ICP	inductively coupled plasma
ICP-OES	inductively coupled plasma optical emission spectroscopy
J	Joule
kg	kilogram
m	metre
MAPE	maleic anhydride-grafted polyethylene
MAPP	maleic anhydride-grafted polypropylene
MFI	melt flow index
MKF	milled kenaf fiber
mL	milliliter

NaOH	sodium hydroxide
NDF	neutral detergent fiber
NFC	natural fiber composite
OH	hydroxyl group
OMAFRA	Ontario Ministry of Agriculture, Food and Rural Affairs
PE	polyethylene
PP	polypropylene
SEM	scanning electron microscopy
SD	standard deviation
$T_{5\% \text{ onset}}$	temperature when 5% mass is lost
TAPPI	Technical Association of the Pulp and Paper Industry
TGA	thermogravimetric analysis
T_{max}	temperature when there is maximum change in rate of mass loss
USA	United States of America
USD	United States dollar

1 Motivation

The automotive sector requires bulk materials that have specific properties. Lighter materials are preferred so that there is greater fuel efficiency and a decrease pollution. The automotive sector is one of the main driving forces in adopting more environmentally friendly materials. In 2011, President Obama set the goal for fuel efficiency to be raised from 36.4 miles per gallon in 2014 to 54.5 miles per gallon for cars for the year 2025 [1], [2].

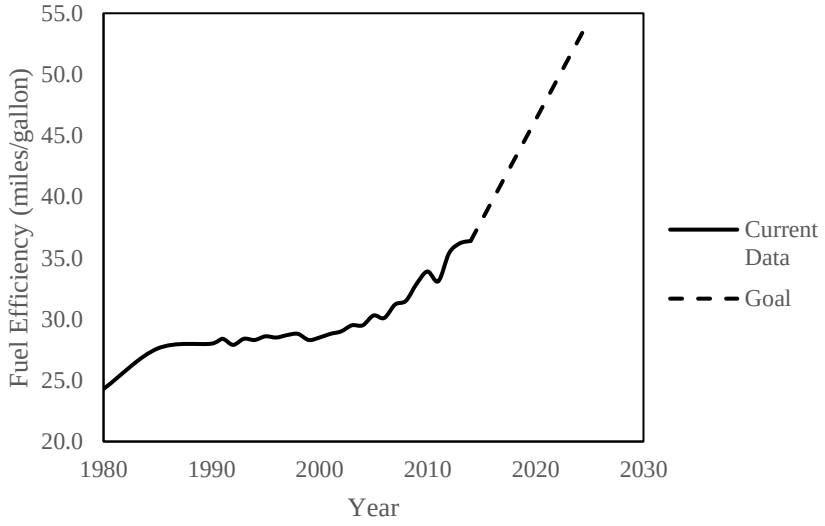

Figure 1: Fuel efficiency for passenger cars in the United States of America [2].

The use of composite materials has grown in the automotive industry. Plastics and composites account for 8% of automotive weight or 334 pounds on average [3]. While this may

seem small, it accounts for approximately half of the vehicle volume [3]. Composite materials can be used in areas such as door panels and bumpers.

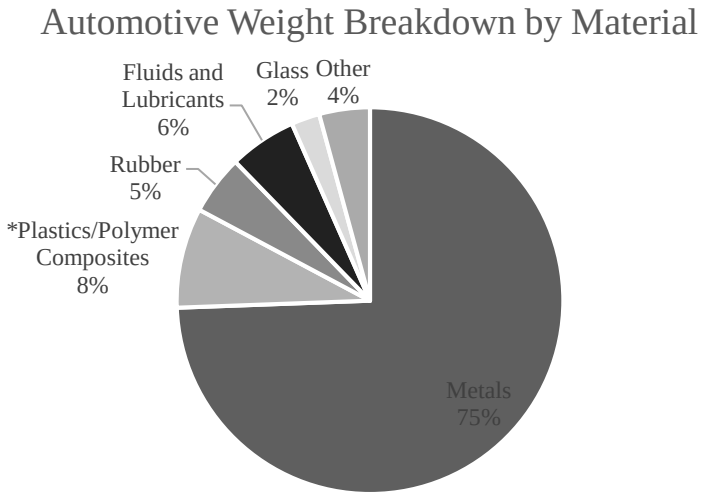

Figure 2: Vehicle material breakdown by weight percentage in 2015 [3].

Materials reinforced with natural fibers are a promising option because they are light. By using natural fibers, it may be possible to reduce the vehicle weight by 30% when substituted for synthetic reinforcing agents like glass fiber [4]. As a result, the use of natural fiber reinforced composites has increased in recent years [5].

2 Objectives

The objective of this research was to assess possible methods for improving natural fiber performance in a polymer matrix. The physical properties of natural fibers can be improved by sodium hydroxide treatment and by the addition of the coupling agent, maleic anhydride [6]. Several studies have shown composite improvement when using these treatments on natural fibers. However, there is a lack of knowledge on the effect these chemical treatments have on the inorganic content of the natural fibers. Inorganic content may influence the natural fiber reinforced composite performance.

This study seeks to examine the native inorganic content of the fiber and understand how the inorganic content changes with sodium hydroxide treatment. The natural fiber selected in this study was kenaf which has a relatively high inorganic content in comparison to other common natural fibers such as hemp and jute [7].

The objectives of this study are:

- Quantify the chemical composition and inorganic content of kenaf fiber after sodium hydroxide treatment
- Determine the effects of sodium hydroxide treatment and maleic anhydride coupling on the mechanical properties of kenaf polypropylene composite

3 Literature Review

This chapter presents the current knowledge of natural fiber reinforced composites. This chapter explains terms used in later chapters as well as background information.

3.1 Natural Fiber Composites

Natural fiber composites (NFC), as the name suggests, typically consists of natural fibers embedded in a matrix, typically polymer based as shown in Figure 3 [6]. Matrices are usually thermoset or thermoplastic depending on the applications and available equipment.

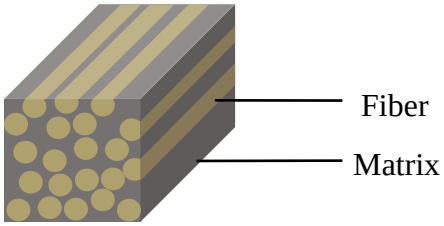

Figure 3: Depiction of natural fiber composite. Fibers are typically embedded in a polymer matrix.

NFCs have been used in many areas as an alternative to synthetic reinforced fibers such as glass fiber composites or carbon fiber composites. Natural fibers possess low density and lightweight properties as compared to glass and carbon fibers, but natural fibers have poorer

mechanical, structural and water stability. Their properties are also dependent on growth conditions [8].

NFCs are used in multiple industries. In 2016, NFCs account for a 4.46 billion USD global market and are expected to have a compound annual growth rate of 11.8% from 2016-2024 as shown in Figure 4 [5]. The growth is driven by an increase need for more environmentally friendly products. This is due to consumers support for environmental protection but, more importantly, policy support from governing bodies. For example, the United States Department of Agriculture has put a plan in place to increase the use of plant based chemical building blocks to 10% by 2020 and 50% by 2050 [9].

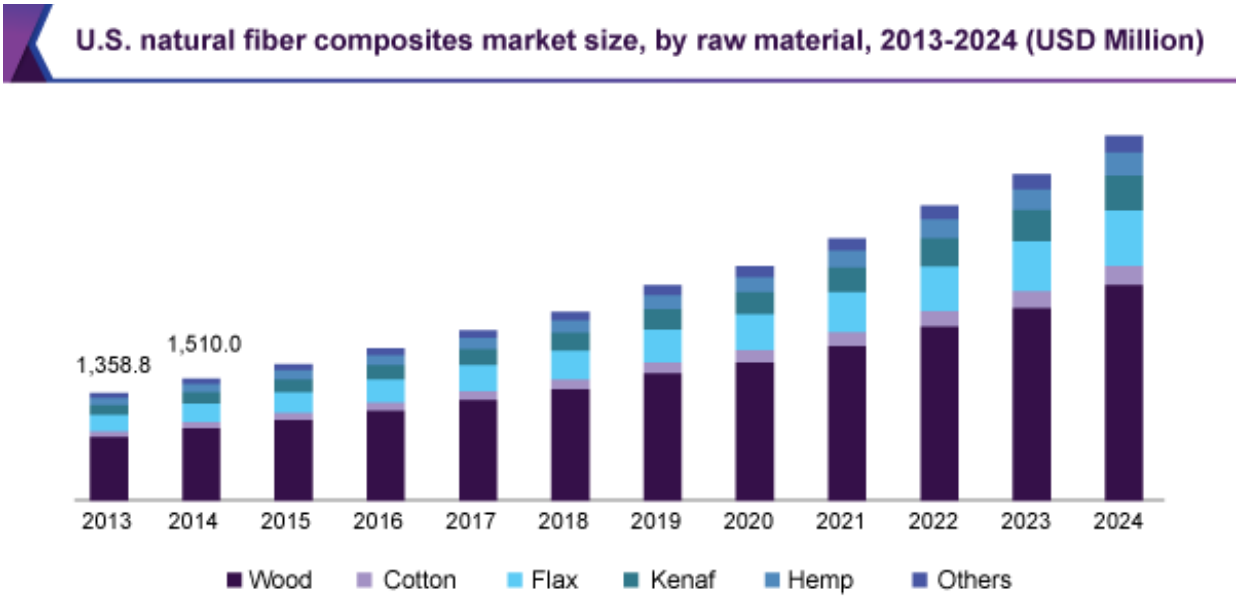

Figure 4: USA market growth of natural fiber reinforced composites [5].

NFCs are most widely used in construction followed by the automotive sector as shown in Figure 5. Key global companies within the automotive sector include FlexForm Technologies LLC and TECNARO GMBH. According to Grand View Research, construction accounted for 56% of the global market share of NFCs in 2015. They are typically used in non-load bearing or non-primary structures such as partition boards, window frames, and ceiling beds [10]. Outside of construction, NFCs can also be used to make electronic cases and bicycles, among other products [5].

The automotive market share accounts for the next highest market share category after construction with a global market share of over 30% in 2015. It is used to make auto parts such as dash boards and seat backs. Figure 6 shows examples of NFCs being used in the automotive sector. NFCs have market penetration because of its ability to reduce automobile weight and therefore improve fuel efficiency. NFCS has the ability to reduce the automobile weight by 30% while reducing manufacturing cost by 20% [5].

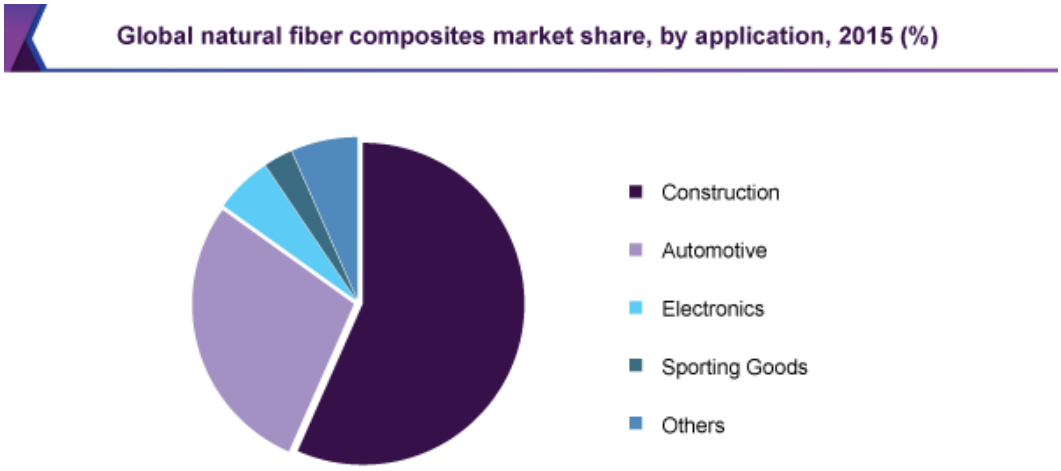

Figure 5: Industrial sectors of natural fiber reinforced composites [5].

Figure 6: Mercedes-Benz E-Class components made from various natural fiber reinforced composites [8].

3.2 Natural Fibers

Natural fibers refer to fibers from non-synthetic or non-man-made sources like plant material. Natural fibers can be classified in three main groups: plant fibers, animal fibers, and mineral fibers as illustrated in Figure 7. Plant fibers can be further divided into wood and nonwood [6].

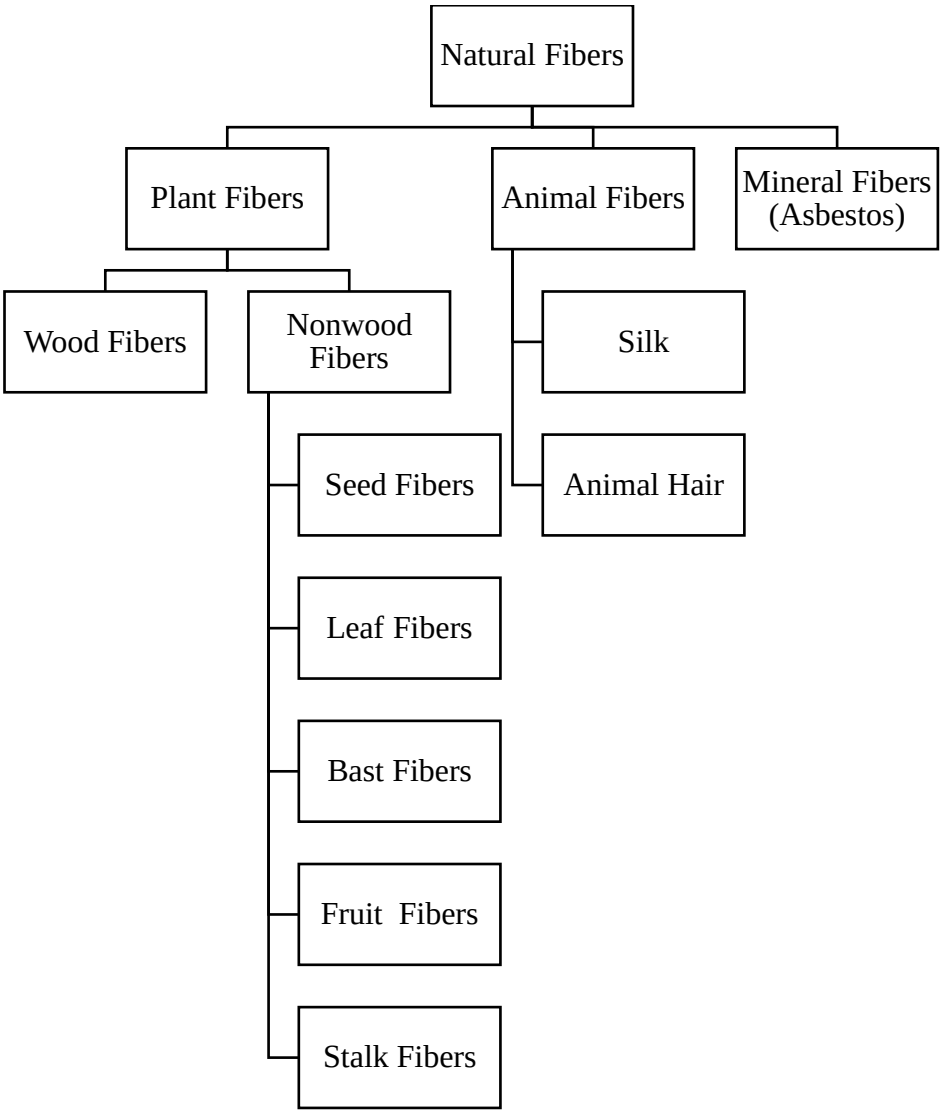

Figure 7: Classification of natural fibers [6].

One of the most common mineral fibers are silicate-based asbestos. Asbestos is not widely used because of the associated health hazards [6]. Animal fibers are mostly protein based such as hair and feathers which are primarily composed of keratin, or silk which is composed of fibroin [11].

Plant fibers have been widely used in composites [8]. Wood is the most common type of plant fiber but non-wood fibers play an important role in reinforcing composites [6]. Non-wood fibers can be further broken down into those isolated from the seed, leaf, bast, fruit, and stalk. Bast fibers are mature fibers sourced from the phloem that surrounds the stem which tend to be stiffer [6]. In the literature, the term natural fiber has been used in a different context than presented in Figure 7 and is typically used to refer to non-wood fibers. Therefore, from this point onwards, natural fibers will be used to refer to non-wood fibers only. Table 1 shows the global production of some common natural fibers.

Table 1: World production of common natural fibers in 2013 [6].

Fiber	**Global Production (10^3 ton)**
Sugarcane bagasse	75,000
Bamboo	30,000
Jute	2,300
Kenaf	970
Flax	830
Grass	700
Sisal	378
Hemp	214

In Canada, the crops grown primarily for fiber for use in composites are flax and hemp [12], [13]. In 2017, there was over 315,000 tonnes of flax fiber produced [12], [13]. The hemp fiber production is lower with over 64,000 tonnes in 2014 [14]. Kenaf is not currently grown for fiber production in Canada but small test crops have been grown successfully. The production of kenaf fiber in Canada is not known.

3.2.1 Plant Fiber Structure

Plant fibers typically have a diameter on the order of 1-100 µm with large variations while fiber length is dependent on the plant specie. The structure of the plant fiber discussed in this section can be used to describe bast fibers of the plant stem but also other types of plant fibers. Plant fibers have a similar structure consisting of a primary cell wall and a secondary cell wall covered by a cuticle [15]. The cell walls are composed of cellulose microfibrils that are randomly oriented. The definition of cellulose microfibril is vague and may vary between publications but generally refer to cellulose fibrils with diameters between 2 and 20 nm [16]. The fiber gets most of its strength from the cellulose component and is usually the main component of the fiber. The cellulose microfibrils are organized cylindrically in layers around a central lumen in the stem which is shown in Figure 8. The angle of the cellulose microfibrils with respect to the fiber axis effects the stiffness and ductility of the fibers. Microfibrils are held together by hemicellulose, lignin, and pectin which act as a glue between the microfibrils [6], [17].

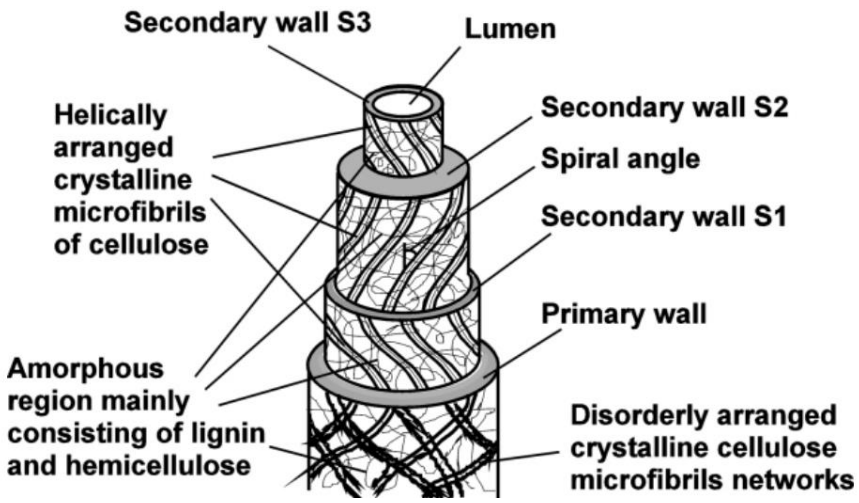

Figure 8. Natural fiber structure showing wall structure and cellulose arrangement [17].

The primary cell wall consists of fibrils that are almost perpendicular to the axis of the fiber. The primary cell wall provides a large amount of structural support to the fiber and maintains its integrity [15]. In the secondary cell wall, the microfibrils become progressively more parallel to the axis of the fiber as they get closer to the lumen. Fibers also become more organized and take on a helical structure [15].

The cuticle covers the microfibrils and is mixed into the primary cell wall. It is composed of pectin, wax, and protein [15]. The lumen is a central hollow tube through the fiber. The lumen is initially filled with liquid but as the fiber ages the lumen dries and may collapse [15].

3.2.2 Composition of Fibers

Fiber composition differs between plant species and will vary with growth conditions such as temperature and soil quality. Table 2 highlights the differences in composition for different types of fibers.

Table 2: Chemical composition of natural fibers.

Fiber	Cellulose (wt. %)	Hemicellulose (wt. %)	Lignin (wt. %)	Pectin (wt. %)	Ash (wt. %)	Source
Bast Fiber						
Kenaf	31-57	21.5-23	8-19	3-5	2-5	[7], [18]–[20]
Jute	45-71.5	13.6-21	12-26	0.2	0.5-2	[7]
Hemp	57-77	14-22.4	3.7-13	0.9	0.8	[7]
Flax	71	18.6-20.6	2.2	2.3	-	[7]
Leaf Fiber						
Sisal	47-78	10-24	7-11	10	0.6-1	[7]
Abaca	56-63	15-17	7-9	-	3	[7]
Henequen	77.6	4-8	13.1	-	-	[7]
Seed Fiber						
Cotton	92	6	0.7-1.6	<1	0.8-2.0	[21], [22]
Milkweed Floss	55	24	18	-	-	[23], [24]
Fruit						
Coconut Coir	32.65	7.95	59.40		5.1	[25]
Stalk						
Rice	37.0	16.5	13.6	-	19.8	[26]
Corn	42.7	23.2	17.5	-	6.8	[25]

Bast fibers have a wide range of composition (31-77% cellulose, 13-23% hemicellulose, 2.2.-26% lignin, 0.2-5% pectin, and 0.8-5% ash). Kenaf fiber has relatively low cellulose (31-57%) high pectin (3-5%), and high ash content (2-5%). Flax has notably low lignin content (2.2%). Bast fibers have been used in composites and have been grown extensively (see Table 1).

Leaf fibers also show variety in their composition (47-78% cellulose, 4-24% hemicellulose, 7-13.1% lignin, 10 % pectin, and 0.6-3% ash). In henequen fibers, hemicellulose is low (4-8%), and lignin is high (13.1%) when compared to other leaf fibers. Of the leaf fibers, pectin is only reported for sisal fibers. The pectin content in sisal fibers (10%) is high compared to all other fibers reported.

In the seed fiber category, cotton has the highest cellulose content (92%), low hemicellulose content (6%), and very low lignin content (0.7-1.6%). Milkweed has low cellulose content (55%) when compared to cotton. Milkweed also has higher hemicellulose content (24%) and lignin content (18%) when compared to cotton. Pectin (<1%) and ash (0.8-2.0%) were reported for cotton only.

In the fruit fiber, coconut coir, cellulose (32.65%) and hemicellulose (7.95%) is low but has the highest lignin content (59.40%). Pectin was not reported for coconut coir. Coconut coir has higher ash content (5.1%) than that reported for bast, leaf and seed fibers.

In the stalk fibers of rice and corn, the cellulose (37.0- 42.7%), hemicellulose (16.5-23.2%), and lignin (13.6-17.5%) are not notably high or low. However, stalk fibers are notable for their high ash content (19.8% in rice, and 6.8% in corn).

The major components of non-wood plant fibers and their role in the fiber's properties and NFCs performance will be discussed in the following sections. The potential for fiber modification, structure, stability, and organization will also be reviewed.

3.2.2.1 Cellulose

Cellulose is responsible for the structural integrity of the fiber. Cellulose can be organized into crystalline (highly ordered areas) and amorphous (weaker, less organized areas) regions. The distribution of crystalline and amorphous regions in cellulose is not well understood. Cellulose is a polysaccharide consisting of glucose units arranged in a linear chain linked by β (1→4) glycosidic covalent bonds. There are hundreds to tens of thousands of glucose units in a cellulose molecule [27]. Intermolecular hydrogen bonds between the chains hold cellulose sheets together to form crystalline cellulose. Cellulose bundles can come together to form small microfibrils which are held together with each other by hemicellulose, lignin and pectin. However, some cellulose will take on an amorphous structure because of the lack of organised hydrogen bonds between cellulose molecules. Cellulose is relatively resistant to chemical degradation in comparison to other molecules present in the plant fiber because of the strong linear β(1→4) glycosidic bonds between the glucose molecules [28]. It can, however, be degraded by acid hydrolysis, alkaline hydrolysis, and enzymatic hydrolysis by cellulase. Cellulose has one primary hydroxyl group and two secondary hydroxyl groups which are available for cellulose modification. The secondary hydroxyl groups are less reactive than the primary hydroxyl groups because of stearic hindrance [27].

3.2.2.2 Hemicellulose

Hemicellulose holds pectin and cellulose together forming a network. Hemicellulose is composed of glycans (D-xylose, mannose, L-arabinose, galactose and glucuronic acid) with branched chains and are typically shorter than 200 units [27]. Hemicellulose is less chemically resistant than cellulose because of its lack of crystalline structure. Hemicellulose molecules are held together with weaker bonds since it lacks strong hydrogen bonds. As a result, it is easily hydrolysed and can be degraded under basic (such as 5% Na_2CO_3) and acidic conditions (such as 2% HCl) [27]. Hemicellulose can be removed from cellulose fiber, as it acts as a weak point due to poor chemical resistance and strength.

3.2.2.3 Lignin

Lignin provides some stiffness and resistance to water for the plant cell and is located between the cellulose, hemicellulose, and pectin fractions. It is composed of cross-linked aromatic groups and does not have a defined primary structure [28]. The primary aromatic subunits of lignin are guaiacylpropane, syringylpropane, and p-hyroxyphenylpropane. These subunits vary in concentration between plant species. Lignin is structured into soluble (amorphous) and insoluble (crystalline) regions formed by hydrogen bonding between hydroxyl groups. Lignin can be digested using basic solutions (such as NaOH) which cleaves ether bonds, neutral nucleophiles HSO_3^- or SO_3^{2-} which break ether bonds, and acidic SO_2 solution which breaks ether bonds and sulfonates the α-carbon [27].

3.2.2.4 Pectin

Pectin connects the plant cells to each other and consists of heterogenous branched polysaccharides (rhamnose and arabinose). It is hydrated because of the galacturonic acid units [28]. Pectin can be degraded in water and be broken down by acidic solutions or pectinase enzyme [27].

3.2.2.5 Ash

Ash represents non-thermally degraded components such as the inorganic constituents of the plant material or fiber [27]. Ash is typically composed of potassium, magnesium, calcium, chlorine, aluminium, and sodium (Table 3). The inorganic constituents will vary between species and their relative composition is influenced heavily by growing conditions as they are absorbed from the soil. The inorganic content exists in the form of ions which are distributed throughout the plant based on their function in plant physiology [27]. The inorganic components play many roles in plants. Ionic channels use potassium and silicon is used to respond to environmental stresses. Calcium aids with cell wall structure and magnesium is found in chlorophyll which is used in photosynthesis [27].

The inorganic content present in plant fibers can also affect the success of fiber processing. Alkalization of fibers often has large amounts of alkali waste at the end of a production cycle. This waste is then postprocessed for reuse or disposal. Excessive amounts of silicon from the fiber will dissolve in alkali waste and make it very viscous which may cause difficulty in waste postprocessing [27]. Transition earth metals can change fiber colour and decompose bleaching agents. This, in turn, reduces bleaching effects and degrades carbohydrates

[27]. In contrast, alkaline earth metals, such as calcium and magnesium, may stabilize lignin and carbohydrates during bleaching processes and combat effects from transition earth metals [27].

Kenaf and cotton both have significant inorganic content with ash representing 2-5% and 5.76%, respectively, of the biomass [7], [19], [20], [21]. They both have relatively large amounts of potassium, calcium, chlorine, and magnesium content compared to other natural fibers. In contrast, hemp has 0.8% ash content while flax has unreported ash content [7]. Table 3 shows lower concentrations of inorganic elements present in flax when compared to hemp [29]. However, the inorganic content reported in Table 3 was obtained using different analytical techniques. For kenaf, neutron activation analysis was used while inductively coupled plasma spectroscopy (ICP) was used for flax and hemp. Cotton inorganic content was determined using both ICP and atomic absorption spectroscopy.

Table 3: Inorganic composition of selected plant fibers.

Elements (ppm)	Kenaf [19]	Cotton [15]	Flax [29]	Hemp [29]
Na	245	100-300	-	365
K	2931	2000-6500	64.1	67.8
Ca	1292	400-1200	310	540
Cl	1533	-	-	-
Al	325	-	76.1	86.8
Mn	28	1-10	-	-
Mg	2801	400-1200	86.6	82.1
Fe	-	30-90	33	34.8

3.2.2.6 Fiber Chemical Analysis

There are common standardized methods to determine the composition of cellulose, hemicellulose, lignin and ash. One of the most common set of references for this analysis comes from the Technical Association of the Pulp and Paper Industry (TAPPI). TAPPI T203 cm-99 is the standard used to determine cellulose and hemicellulose content based on the solubility of the compounds in various solvents. TAPPI T222 om-02 is used to determine lignin content based on the fact that lignin has resistance to sulfuric acid. TAPP T 211 om-02 is used to determine ash by combustion of the fiber at elevated temperatures [30]. ANKOM Technology methods have also been used to determine major component concentration. Standards (A2000) use the same principles as the TAPPI standards above except the equipment and solvents used in ANKOM

Technology methods are different [31]. Table 4 shows the composition of kenaf fibers obtained from both TAPPI and ANKOM Technology methods.

Table 4: Component concentrations of kenaf fibers using standard methods.

Kenaf	Location	Preparation	Cellulose (wt. %)	Hemicellulose (wt. %)	Lignin (wt. %)	Total Ash (wt. %)	Method	Source
Bast	Iowa, USA	Milled to 2mm with Wiley mill	69.2	19.4	5.5	5.9	ANKOM	[32]
Bast	Malaysia	Milled with PFI mill	63.5	17.6	12.7	2.2	TAPPI	[33]
Bast	Malaysia	-	56.4	26.2	14.7	2.2	TAPPI	[19]
Core	Italy	Milled with 0.5 mm by 30mm sieves in a cutting mill	35.0	15.0	21.3	-	TAPPI	[34]
Bast + Core	Malaysia	Grinded to 0.250-0.420mm with a mechanical grinder	37.3	51.8	14.4	4.7	TAPPI	[35]

3.2.3 Mechanical Properties

Mechanical properties of importance to fibers and composites will be reviewed here. Tensile stress is a uniform force that is applied perpendicular to the surface so that it stretches atoms. Stress (σ) can be defined by equation (1).

$$\sigma\ (Pa) = \frac{P_n(N)}{A(m^2)}$$

(1)

where P_n is the applied load normal to the surface, and A is the cross-sectional area [36]. When tensile stress is applied to a NFC, failure is common because of poor compatibility between filler and matrix. Strain (ε) is the ratio between length (δ) and the original length (L_0). Elongation at break is the strain at the point a material fails expressed as a percentage [37]. By plotting stress vs strain in a stress-strain curve, the Young's modulus, E, can be obtained by the slope of the linear portion of the curve [36]. To determine tensile properties, a standard from the American Society for Testing and Materials (ASTM-D638) can be used. The composite sample has a controlled load attached and the displacement between the clamps holding the sample is measured. Typically, the change in length for a given applied load is measured and outputted by a testing machine. This information can then be used to estimate the tensile strength, Young's modulus and elongation at break.

Mechanical properties of the fibers, such as tensile strength and elasticity, are specific to the specie. Typical mechanical properties of natural fibers are compared to synthetic fibers in Table 5. Synthetic fibers shown for comparison are E-glass, S-glass, and carbon fiber. E-glass and S-glass are classes of glass fibers. E-glass is commonly used for electrical applications. S-glass is more expensive and is used for applications which require high strength. The tensile strength is defined as the maximum stress that a material can bear before failure in the direction that elongates the material [36]. The tensile strength of bast fibers ranges between 345-1500 MPa, higher than that of sisal fiber and cotton fiber, but lower than that of synthetic fibers.

Kenaf, jute, hemp and flax fibers are relatively comparable in tensile strength. The tensile strength of kenaf fiber is 2-4 times lower than that of synthetic fibers.

The Young's Modulus is defined as the proportion of stress per strain of a material [36]. The Young's Modulus of bast fibers ranges between 10 to 80 GPa, higher than that of sisal and cotton fiber, but lower than that of synthetic fibers. The Young's Modulus of kenaf fiber is higher than jute fiber but lower than hemp and flax fiber. The Young's Modulus of kenaf fiber is 2 to 5 times lower than that of synthetic fibers.

The elongation at break represents the ratio of the length of the material at failure to the original length of the material [37]. The elongation at break for bast fibers ranges between 1.2 and 3.2% which is lower than that of sisal and cotton fiber but similar to synthetic fibers. The density of bast fiber, which ranges between 1.3 and 1.5 g/cm^3, is similar to sisal, cotton and carbon fibers, but lower than E-glass and S-glass. The density of bast fiber is about half that of E-glass and S-glass. While mechanical properties are the primary limitation with the use of natural fibers in composite materials, their thermal stability and poor water resistance limit their use in automotive and construction applications [38], [39].

Table 5: Mechanical properties of natural and synthetic fibers.

Fiber	Tensile Strength (MPa)	Young's Modulus (GPa)	Elongation at Break (%)	Density (g/cm^3)	Sources
Bast Fiber					
Kenaf	930	53	1.6	1.45	[40], [41]
Jute	393-800	10-30	1.5-1.8	1.3-1.46	[7]
Hemp	550-900	70	1.6	1.48	[7]
Flax	345-1500	27.6-80	1.2-3.2	1.4-1.5	[7]
Leaf Fiber					
Sisal	400-700	9.0-38.0	2.0-14	1.33-1.5	[7]
Seed Fiber					
Cotton	287-597	5.5-12.6	3.0-10.0	1.5-1.6	[7]
Synthetic Fiber					
E-glass	2000-3500	70	2.5-3.0	2.5	[7]
S-glass	4570	86.0	2.8	2.5	[7]
Carbon (standard)	4000	230.0-240.0	1.4-1.8	1.4	[7]

3.2.4 Kenaf

Kenaf (*Hibiscus cannabinus*) is a promising crop with good mechanical properties compared to other bast fibers (hemp and flax), and superior characteristics compared to sisal and cotton fibers (Table 2 and Table 6). Physical properties of bast fibers are shown in Table 6. However, kenaf has high ash content when compared to other bast fibers. The high ash content of kenaf fibers may be difficult to process and cause premature wear of equipment during processing but kenaf can potentially be modified to improve its properties using chemical and mechanical treatments.

Table 6: Physical properties of bast fibers.

Fiber	Length (mm)	Diameter (µm)	Micro-fibrillar Angle (°)	Moisture Content (wt. %)
Kenaf	01.62-3.89 [19]	12.17-47.85 [19]	9-15 [44]	8-16 [45], [46]
Hemp	15-25 [6]	22-25 [6]	2-6.2 [6]	6.2-12 [6]
Flax	4-77 [6]	5-76 [6]	5-10 [6]	8-12 [6]

The range of physical properties for kenaf, hemp and flax speak to the diverse nature of the composite materials that could be produced with these fibers. The length and diameter characteristics will play a role in determining the amount of stress that can be transferred in a composite. Kenaf is the shortest of the bast fibers. The micro-fibrillar angle helps to determine the fiber strength. A smaller angle typically results in higher tensile strength while a larger angle

typically results in greater ductility [47]. The moisture content can speak to the hydrophilicity of the fiber.

Kenaf is currently not widely grown in Canada. It is typically grown in temperatures above 10°C and the growth period lasts for four to five months [48]. This limits growth of kenaf in Canada to mid-spring to early fall since other times may drop below 10°C. Companies such as Goldco International Incorporated have invested resources in making kenaf a Canadian crop. They have performed agronomy studies in partnership with the University of Guelph which determined kenaf can be grown in Ontario with high yield and good quality. The study produced 7,000-19,400 kg/ha (depending on farm location) in 2012 [49]. These values are comparable to kenaf grown in USA and Malaysia (2,500-18,000 kg/ha) [48]–[50]. This can be compared to the 1460 kg/ha for hemp and 750-5,000 kg/ha for flax which are common crops in Canada [12], [14] as shown in Table 7.

Kenaf is a suitable crop for Canada because of its adaptability to various environments and its resistance to disease and pests. It is a very hardy plant that can be grown in various environments as it needs little soil minerals and is adaptable to range of sunlight exposure and water levels. It is resistant to most diseases and infections. When kenaf crops are reaped, the leaves are left behind adding nitrogen back into the soil [48]. Kenaf is a suitable crop to include into crop rotation because of its crop density and yield. The CO_2 emissions associated with a crop is an indicator of the environmental impact of the crop as CO_2 is one of the major greenhouse gases produced in agriculture. Kenaf has the lowest farm to fiber CO_2 emissions produced (579 kg CO_2/t fiber) when compared to hemp and flax where the CO_2 emissions

include those associated with field operations, seeds, fertilizer, fertilizer emissions, pesticides, transportation from field to processing area, and fiber processing [51].

Table 7: Growth and production comparison for kenaf, hemp and flax.

Property	Kenaf [48]–[51]	Hemp [14], [51]	Flax [12], [51]
Chemical Treatments	Fertilizer	Fertilizer	Fertilizer, fungicide, insecticide
Environmental Conditions	Warmer climate, well-drained soils	Colder climate, well-drained soil	Colder climate, clay soils
Plant Fiber Yield	2,500-19,400 kg/ha	1,460 kg/ha	750-5,000 kg/ha
Farm to Fiber CO_2 Emissions	579 kg CO_2/t fiber	768 kg CO_2/t fiber	732 kg CO_2/t fiber

3.2.5 Fiber Extraction

As indicated earlier, the use of natural fibers for industrial applications is limited by the lower strength and thermal stability, as well as poor compatibility with the hydrophobic matrix. The limitations in strength and thermal stability can be partially addressed by removing hemicellulose and lignin while retaining the cellulose component. A variety of extraction techniques have been developed and can be broadly classified as chemical, physical, enzymatic and biological. The review of fiber extraction techniques will be limited to chemical techniques, namely alkaline, maleic anhydride, and silane treatments.

3.2.5.1 Alkali Treatment

Alkali treatment is a common treatment used to improve fiber-matrix interaction and improve dispersion of the natural fiber in the matrix. The fiber is soaked in a sodium hydroxide (NaOH) solution and then rinsed and dried. One of the major benefits of alkali treatment is the removal of impurities (hemicellulose, lignin, pectin, and waxes) present in the fiber bundle as shown in Table 8. With alkali treatment of kenaf, hemp, and flax the cellulose content increases while hemicellulose and lignin content decreases.

Table 8: Bast fiber composition with varying NaOH treatments.

Fiber	[NaOH] (%)	NaOH Temper-ature (°C)	Treat-ment Time (minutes)	Cellulose (%)	Hemi-cellulose (%)	Lignin (%)	Ash (%)
Kenaf [33]	-	-	-	63.5	17.6	12.7	2.2
Kenaf [33]	15% (and 1% anthra-quinone)	160	105	81.5	12.7	2.5	-
Hemp [52]	-	-	-	76.12	12.28	5.65	-
Hemp [52]	5%	RT	30	83.63	7.49	2.61	-
Hemp [52]	5%	boiling	30	89.16	1.93	2.07	-
Flax [53]	-	-	-	75.81	7.84	4.03	-
Flax [53]	18%	RT	60	92.33	3.44	1.12	-

There are many weak points present in non-cellulosic material such as hemicellulose and lignin. The relationship between cellulose and other main components is shown in Figure 9. Alkali treatment removes hemicellulose, lignin, pectin, oil, and wax from fibrils and leaves a cleaned cellulose surface. This reduces the diameter of the fiber and increases the aspect ratio [54].

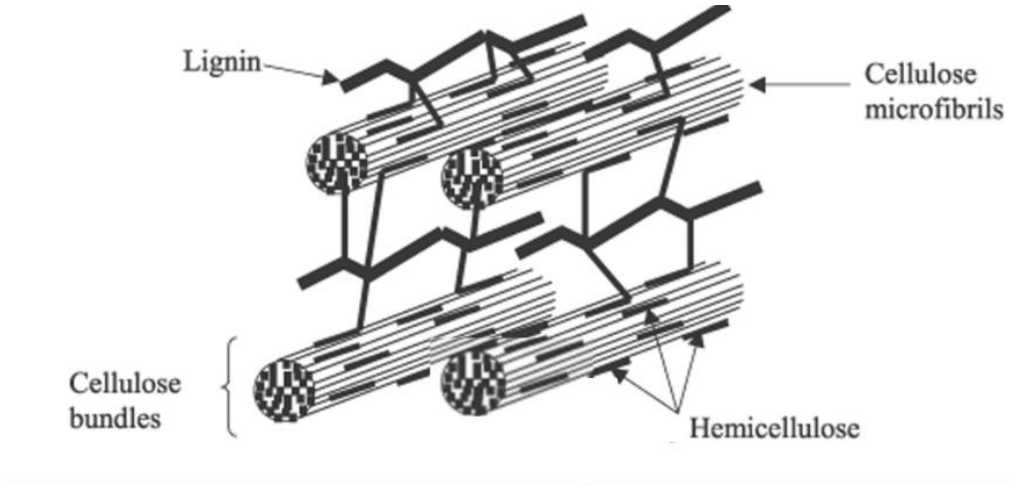

Figure 9: Closer look at natural fiber structure showing relationship between fiber components [55].

The removal of impurities (hemicellulose, lignin, pectin, and waxes) from the fiber, improves the stress transfer capacity between cells. Mechanical and thermal properties of composites are also improved because of the increased adhesion between fiber and matrix. However, excessive alkali treatment can cause a reduction in mechanical properties of the fiber [54]. Alkalizing the plant-based fiber also can cause a change in the cellulose structure by removal of hydrogen bonds holding cellulose in the crystalline formation. An amorphous region

is formed by changing the orientation of the crystalline cellulose thus causing cellulose chains to be less tightly packed. The amorphous region allows more access for further chemical treatments of the fiber and nucleation sites for the polymer but allows water to fill the gaps of the amorphous region [54].

Cellulose has several free hydroxyl groups on its surface. When treated with sodium hydroxide, hydroxyl groups are hydrolyzed and replaces hydroxyl groups with O-Na. This results in a cellulose-O-Na structure as shown in

(2). The removal of hydrophilic OH groups helps to improve the moisture resistance of the fiber and therefore reduce the effect of moisture absorption caused by formation of amorphous regions [54].

$$\text{Fiber} - \text{OH} + \text{NaOH} \rightarrow \text{Fiber} - \text{O} - \text{Na} + \text{H}_2\text{O}$$

(2)[7]

Optimal NaOH treatment conditions, NaOH concentration, temperature and duration, have an important impact on the resulting fiber performance. If conditions are too severe, degradation of the cellulose bundles will take place which negatively affects the performance in a composite. Edeerozey et al. compared the effect of NaOH conditions on kenaf fibers. In their study, NaOH solutions at room temperature and 95°C with concentrations of 3%, 6%, and 9% were used. The 3% NaOH treatment was insufficient for removing impurities as shown by bumpy morphology obtained from scanning electron microscopy (SEM). The 9% NaOH treatment cleaned kenaf the best as shown by morphology without bumps obtained from SEM. However, 6% NaOH treatment solutions at 95°C (243.7 N/mm^2), followed by 6% NaOH

treatment at room temperature (293.3 N/mm^2) had the best results for unit break of the fiber when compared to untreated (215.4 N/mm^2), 3% NaOH treatment at room temperature (219.4 N/mm^2), and 9% NaOH treatment at room temperature (165.0 N/mm^2) [56]. Mwaikambo and Ansell showed that for hemp, sisal, jute and kapok fibers, 6% NaOH treatment concentration gave best results for cleaning the fiber of impurities while maintaining a high index of crystallinity [22].

3.2.5.2 Maleic Anhydride

The coupling agent maleic anhydride is generally used in maleic anhydride-grafted polypropylene (MAPP). Maleic anhydride reacts with the hydroxyl groups on the surface of the fiber and replaces hydroxyl groups with the MAPP. This results in the fiber being coated with long hydrophobic polymer chains. This improves compatibility with the hydrophobic matrix by forming carbon-carbon bonds which improve fiber wettability and interfacial adhesion [54]. The reaction mechanism is shown in Figure 10.

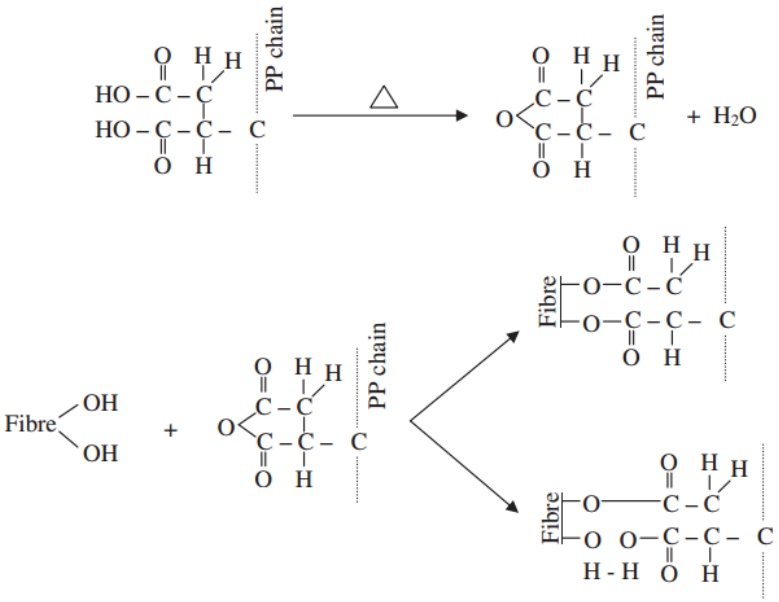

Figure 10: Mechanism of maleic anhydride as a coupling agent for polypropylene and natural fiber cellulose [54].

3.2.5.3 Silane

Silane treatments have been used to improve NFC performance. Silane is a bifunctional molecule and, similarly to MAPP, acts as coupling agent and forms a siloxane bridge between the natural fiber and the polymer matrix [57]. Various types of silanes exist. The type of silane depends on the natural fiber and matrix chosen. The most established type of silane is trialkoxysilane which may have a reactive organofunctionality which binds to the matrix or non-reactive alkyl group which binds to fiber. Common organofunctionalities used are amino, methacryloxy, mercapto, vinyl, and glycidoxy with amino being the most extensively reported [57].

3.3 Composite

Composites generally consist of a polymeric continuous phase (matrix) and a dispersed phase. Typical polymer matrices can be classified according to their source, non-renewable and renewable. Non-renewable polymers generally come from petroleum-based sources such as polypropylene. Renewable polymers come from a source that is readily replenished such as polylactic acid. Similar classification can be used for the dispersed phase, synthetic (such as glass fiber) and natural (such as kenaf). In the context of composites containing a dispersed phase of natural origin, the matrix is limited to polymers that are able to be processed at relatively low temperatures as non-wood plant fibers will degrade at temperatures above 230°C [38]. The polymer matrix is usually either a thermoset or thermoplastic. Common thermosets include epoxy and polyester. Thermoplastics, on the other hand, are melted and cooled into a solid in a reversible process. Common thermoplastics include polypropylene and polyethylene. The type of polymer will also limit processing techniques for the composite production [61].

3.3.1 Polypropylene

Polypropylene (PP) is commonly used as the matrix for natural fiber composites in the automotive sector to make parts such as door panels, floor panels, and underbody panels [8]. In 2016, polypropylene accounted for 25% of plastic used in a vehicle in USA and Canada [58]. Polypropylene is produced in high volume for relatively low costs by polymerizing propylene. Polypropylene is a semi-crystalline polymer. Polypropylene exists as three different stereoisomers (isotactic, syndiotactic, and atactic) depending on the location of the methyl group.

Atactic polypropylene has low crystallinity (5-10%) when compared to isotactic (30-60%) and syndiotactic (30%). Isotactic is the most common commercially available polypropylene as a result of its high crystallinity [59].

Polypropylene has a melting temperature between 160 and 176°C and a glass transition temperature of -30°C. Polypropylene is suitable for use with natural fillers since its melting temperature is below the temperature at which natural fillers typically degrade (~ 230°C). Therefore, PP can be processed below the natural filler degradation temperature. Polypropylene's density is between 0.899 and 0.920 g/cm^3. It has a tensile strength between 26 and 41.4 MPa and elongation of 15% to 700% [8], [60]. The structure of polypropylene is shown in Figure 11.

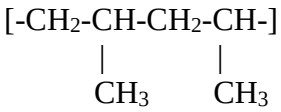

Figure 11: Structure of polypropylene [60].

3.3.2 Dispersed Phase-Matrix Interactions

The interaction between the dispersed phase and the matrix is of utmost importance in a natural fiber composite (NFC) as stress is transferred between the dispersed phase and the matrix at the interface. It is at the interface that composites tend to fail as a result of poor interaction since the natural dispersed phase tends to be hydrophilic and the matrix tends to be hydrophobic.

As a result, the wettability of the dispersed phase by the matrix is of importance to ensure the absence of interfacial defects [62].

Bonding between the dispersed phase and the matrix is a result of mechanical interlocking, chemical bonding, and inter-diffusion bonding. In the case of fibers, their roughness tends to increase mechanical interlocking. Chemical bonding will exist when there will be reactive groups between the fiber and the matrix [62]. This can be achieved by using coupling agents. Inter-diffusion bonding exists when interactions between molecules at the interface such as polymer entanglement will be present [62]. All these mechanisms work together to improve interfacial adhesion between the dispersed phase and the matrix which in turn could give stronger composites.

Failure between the dispersed phase and the matrix may occur through different propagation mechanisms and regions: through the matrix, through the dispersed phase, and through the dispersed phase-matrix interface [63]. If there are weak dispersed phase-matrix interactions, then stress will concentrate at the tip of the crack and causes the dispersed phase to detach from the matrix. If there are strong dispersed phase-matrix interactions, the dispersed phase may break before the matrix. The composite will become brittle and fail perpendicular to the direction of the stress. The propagation of the crack is determined by which of the three regions (matrix, dispersed phase or interface) is the weakest. In order to improve the composite mechanical performance, the optimal path for crack propagation should be through the matrix but close to the surface of the dispersed phase. This occurs because of optimal bonding that absorbs energy but still achieves good interfacial stress transfer [63].

3.3.3 Natural Fiber Composites

Natural fiber reinforced composites are generally obtained by extrusion and injection moulding, and compression moulding.

3.3.3.1 Extrusion

The purpose of extrusion is to mix and homogenize the material mixture. Depending on the extruder used, the material is limited by viscosity at the desired temperature. In NFCs this may limit the amount of fiber that is added as an increase in fiber may increase viscosity in the extruder. A screw extruder typically has one or two screws in a chamber. A single screw extruder has one screw that pushes material through the screw threads of the extruder. Similarly, a twin screw extruder also pushes material through the threads but there are two intertwined screws instead of one, leading to improved mixing. As the chamber is heated and the screw (or screws) turn, material can be added to the chamber through a hopper. This heats the material under pressure and causes it to move through the extruder. As the material moves through the extruder, melting and mixing of the polymer matrix occurs and the filler is incorporated into the melt. After a desired melt volume is reached the composite mixture is pushed outwards. Temperature and screw speed are the main process variables during extrusion. Temperature is typically dictated by the nature of the material. Screw speed determines how long the material will be held inside the extruder. Too long and the material becomes exposed excessively to high temperatures but too short and the material may experience increased shear from increased screw speed which may affect filler properties such as shape [8].

3.3.3.2 Injection Moulding

Injection moulding is used to convert the extruded material into a desired shape. This is done with the aid of heat and pressure. The material from the extruder may be loaded into the heated injection moulder and then melted. The material is then pushed into the mould, typically by screw or pestle. Once in the mould, the material will cool but shrinkage may occur if temperature and pressure settings are not optimal. This can lead to voids in the moulded material [8], [64].

3.3.3.3 Mechanical Properties

The mechanical properties of natural fiber composites have received the most attention since the properties of these materials are generally lower than conventional composite materials. In this section, representative publications of the mechanical properties of natural fiber composites will be reviewed. Subasinghe and Bhattacharyya produced a composite with 30 wt% untreated kenaf bast fibers and 70 wt.% PP obtained by twin-screw extrusion and injection moulding. The tensile strength was approximately 48 MPa (estimates from a figure using plot digitizer) [65]. Ichazo et al. prepared a 40% untreated wood flour (mahogany, cedar, pine, oak and saki-saki) and 60% PP composite through twin-screw extrusion and injection moulding. The addition of wood flour improved the tensile strength from 25 MPa to 37 MPa while the elongation at break decreased from 23.4% to 3.1% [66].

Meon et al. prepared kenaf-PP and kenaf-PE composites with maleated polypropylene (MAPP) and maleated polyethylene (MAPE). Kenaf fibers were treated with 3%, 6% and 9% NaOH solutions. The ratio of kenaf: polymer matrix: maleated polymer was 30:67:3 by mass.

The composite was prepared by compression moulding the mixed materials. The PP-MAPP based composites containing 6% NaOH treated kenaf fibers had highest values for tensile strength by giving a 0.4% increase in its performance. The tensile strength of the composites containing 9% NaOH treated kenaf fiber decreased because of the damage done to the fiber at high concentrations [67].

Kuo et al. used 47% wood flour (spruce, fir and pine mixture) treated with 8% NaOH solutions, 47% PP, 3% MAPP, and 3% zinc stearate to prepare a composite by injection moulding. The NaOH treatment of the wood flour resulted in a 24% increase in tensile strength and a 16% increase for the modulus of rupture [68].

Hosseinaei et al. used 48% wood flour (pine), 50% PP, and 2% MAPP to prepare composites by twin screw extrusion and injection moulding. The addition of MAPP increased tensile strength by 43% and the strain at maximum load by 26% [69].

Sever et al. used alkalized jute fabrics immersed in a 0.3% silane coupling agent solution, and polyester to produce a composite. The silane treatment increased the tensile modulus, tensile strength, elongation at break, flexural modulus and flexural strength (Table 9).

Table 9: Effect of silane treatment on the mechanical properties of jute-polyester composite[70].

Silane Treatment	Tensile Modulus (GPa)	Tensile Strength (MPa)	Elongation at break (%)	Flexural modulus (GPa)	Flexural strength (MPa)
-	28.0	4.0	8.5	12.7	-2.3
0.3%	44.8	56.6	65.3	67.5	28.0

The effect of inorganic nanoparticle impregnation may be used to improve filler-matrix interaction and the mechanical properties. The presence of inorganic constituents at the filler surface may act as a heterogenous nucleation site to initiate the melted semicrystalline polymer matrix to take on the crystalline form [71]. This approach was investigated by Shi et al. where kenaf was impregnated with calcium carbonate particles and improved kenaf-PP composites by 10.4% for tensile strength and 25.9% for tensile modulus [71].

3.4 Characterization Techniques

3.4.1 Thermal Stability

Thermogravimetric analysis (TGA) consists in the use of controlled temperature conditions and the monitoring of the mass change [72]. Samples are purged with a gas such as nitrogen or air depending on if oxidation reactions are required or not. TGA has been used to observe physical and chemical changes of NFCs which include absorption, adsorption,

desorption, decomposition, degradation, chemisorption, desolvation and solid-gas reactions [72]. TGA analysis has also been used to observe changes of key components present in natural fibers. Yang et al. performed TGA analysis on the main components of plant natural fibers: cellulose, hemicellulose and lignin of unknown source. The thermal degradation for each component is shown in Table 10 under a nitrogen environment at 10°C/min.

Table 10: Thermal degradation range of isolated main components of plant fiber [73].*

Component	Temperature Range (°C)	Maximum Mass Loss Rate (wt.%/°C)	Maximum Mass Loss Rate Temperature (°C)	Remaining Residue at 900°C (wt.%)
Hemicellulose	220-315	0.95	268	20
Cellulose	315-400	2.84	355	6.5
Lignin	-	<0.14	-	45.7

*Nitrogen at a flow rate of 120 mL/min of 10°C/min from room temperature to 900°C. Temperature range was obtained from the base of peaks of the differential thermogravimetric (DTG) curve.

The analysis indicates that hemicellulose degrades at a lower temperature range (220-315°C) than cellulose (315-400°C). As lignin degraded slowly across the temperature range investigated in the study, no peak on the DTG curve could be identified. Lignin also has a high residual mass at 900ºC. TGA can be used as a reliable method for observing the removal of hemicellulose by observing the change in mass between 220 and 315°C.

TGA has been used to characterize bast fibers. The TGA analysis and the DTG curve of kenaf and hemp under nitrogen showed a shoulder for hemicellulose followed by a peak for cellulose and finally a high temperature lignin tail [74]. The onset of decomposition was at 219°C for kenaf with a weight loss of 4.9% and 205°C for hemp with a weight loss of 3.1%. Maximum decomposition rates occurred at 284°C for kenaf with a weight loss of 42.9% and 282°C for hemp with a weight loss of 38.2%. At the end of the heating cycle (800°C) the residual mass was 22.4 wt.% for kenaf and 24.6 wt.% for hemp [74].

Dong et al. used TGA to characterize flax fibers under nitrogen. In the DTG curve, there was an initial peak which corresponds with water loss below 100°C. This was followed by a peak between 340°C and 370°C with a maximum decomposition rate at 347°C. This peak corresponds with cellulose loss. There was a residual mass of 21.51% at the end of heating cycle (900°C) [75].

3.4.2 Optical Microscopy

Optical microscopy uses a series of lenses and visible light to produce a magnified image. It is the most common form of microscopy because of its wide availability and affordability. Optical microscopy can be used to observe fiber morphology such as protrusion formation and shape [76]. This is useful as chemical and physical treatments can modify fiber morphology. For example, alkali treatment may roughen the fiber surface [77].

Yussuf and Hassan used optical microscopy to observe the fibrillar nature and high aspect ratio of untreated kenaf [76]. Hughes et al. used optical microscopy to observe kinks and defects in untreated hemp and untreated flax [78]. Arbelaiz et al. observed increased surface roughness and reduced surface impurities (pectin and hemicellulose) of flax fibers soaked in 20 wt% NaOH treatment for one hour at room temperature using optical microscopy [77].

3.4.3 Scanning Electron Microscopy and Energy Dispersive X-Ray Spectroscopy

Unlike optical microscopy which uses visible light to obtain an image, scanning electron microscopy (SEM) uses electrons. An electron gun is focused on the sample which then emits secondary electrons and X-rays that can be converted into an image [79]. This image can be magnified up to 500,000 times with distances between 5 and 10 nm [79]. SEM will produce images with greater detail and magnification than optical microscopy. Since natural fibers and polymer matrix are non-conductive, the SEM imaging of these materials require a sputter coating with conductive material such as gold prior to imaging [79].

Similarly to optical microscopy, SEM may be used to characterize fiber morphology after treatment. It may also be used to observe filler-matrix interaction and material failure modes of the composites. The wettability of the fiber can be investigated by observing the proximity between the fiber and the matrix. For complete wettability, there would be no visible gap

between the fiber and the matrix. This would indicate a smaller contact angle and potentially improved mechanical performance [80]–[82].

Energy dispersive X-ray spectroscopy (EDS or EDX) can be used in conjunction with SEM by analyzing the same emitted X-rays. EDX is able to quantify the elemental makeup of the sample being analyzed. Each element has a specific X-ray emission which can produce a peak when scanned. This phenomenon can be used for elemental mapping of the material. EDX has the ability to scan the surface of the material typically to a depth of 1-2 μm [83].

SEM and EDX have been used to characterize natural fibers and natural fiber composites. Liu et al. performed SEM on a single untreated kenaf fiber to observe the general fiber morphology and on kenaf fiber reinforced soy based biocomposite to observe the morphology of the composite fracture. SEM was used to show the kenaf fiber orientation and interaction between the kenaf fiber and matrix. Kenaf fibers were smooth indicating poor fiber-matrix interaction and is a measure of the extent of fiber pull out [84]. SEM has also been used to observe hemp fibers and hemp-PP composites. Pracella et al. found that ground untreated hemp fibers displayed rough morphology and had an average length of 275 μm. After NaOH treatment, hemp fiber was seen to have a clear fibrillar structure. Hao et al. also performed SEM on hemp-polypropylene composites which showed poor interaction between hemp and PP as well as fiber pull out [85]. Baley used SEM and showed that flax fibers take on a polygonal shape and had defects (kink bands) perpendicular to the direction of the fiber. SEM of the flax-PP composite showed fiber directionality and distribution [86]. EDX mapping of untreated kenaf fibers was

used to quantify its carbon (62.5 wt.%), oxygen (35.27 wt.%), and nitrogen (1.01 wt.%) content [20].

3.4.4 Inductively Coupled Plasma Optical Emission Spectroscopy

Inductively coupled plasma optical emission spectroscopy, ICP-OES (or ICP for short), is often used for elemental analysis. During ICP analysis, a sample is nebulized, and plasma is used to excite the atoms of the sample. The atoms then return to a low energy position and release energy as emission rays [87]. The emission ray is unique for each element and its intensity indicates its concentration [87]. The main benefit of ICP is the very high sensitivity and its ability to analyze multiple elements at once with small amounts of sample. The limit of detection depends on the element and the limit of detection is typically on the order of magnitude of 10 ppm [88]. However, ICP requires sample preparation, is expensive, and spectral interferences may occur [89]. ICP has been used for elemental analysis of natural fibers (cotton, flax, hemp and wool) by Rezic et al. Fibers were microwave digested with 7 mol/L nitric acid (Table 11). Major elements observed were Al, Ca, Fe, K, Mg, Na, Sn, and Zn. K, Mg and Zn content was high and Al, Ca, Fe content is low in cotton compared to other fibers while hemp has large amounts of Al, Fe and Na compared to other fibers. Wool was high in Ca and Sn content and low in K, Mg and Zn content compared to the other fibers analyzed.

Table 11: ICP elemental analysis for natural fibers [29].

Element (mg/g)	Cotton	Flax	Hemp	Wool
Al	13.9	76.1	86.8	25.2
Ba	-	-	-	4.8
Be	0.4	-	-	-
Ca	230	310	540	660
Cr	4.2	-	-	3.1
Cu	-	9.6	0.8	-
Fe	14.4	33.0	34.8	19.3
K	1170.2	64.1	67.8	16.9
Mg	397.3	86.6	82.1	-
Na	-	-	365	-
Ni	3.0	-	-	2.3
Pb	-	-	-	0.7
Sc	-	-	-	5.6
Sn	17.4	-	-	31.6
Zn	14.2	7.2	1.1	-

4 Materials and Methods

A schematic overview of the experimental approach used in this thesis is shown in Figure 12.

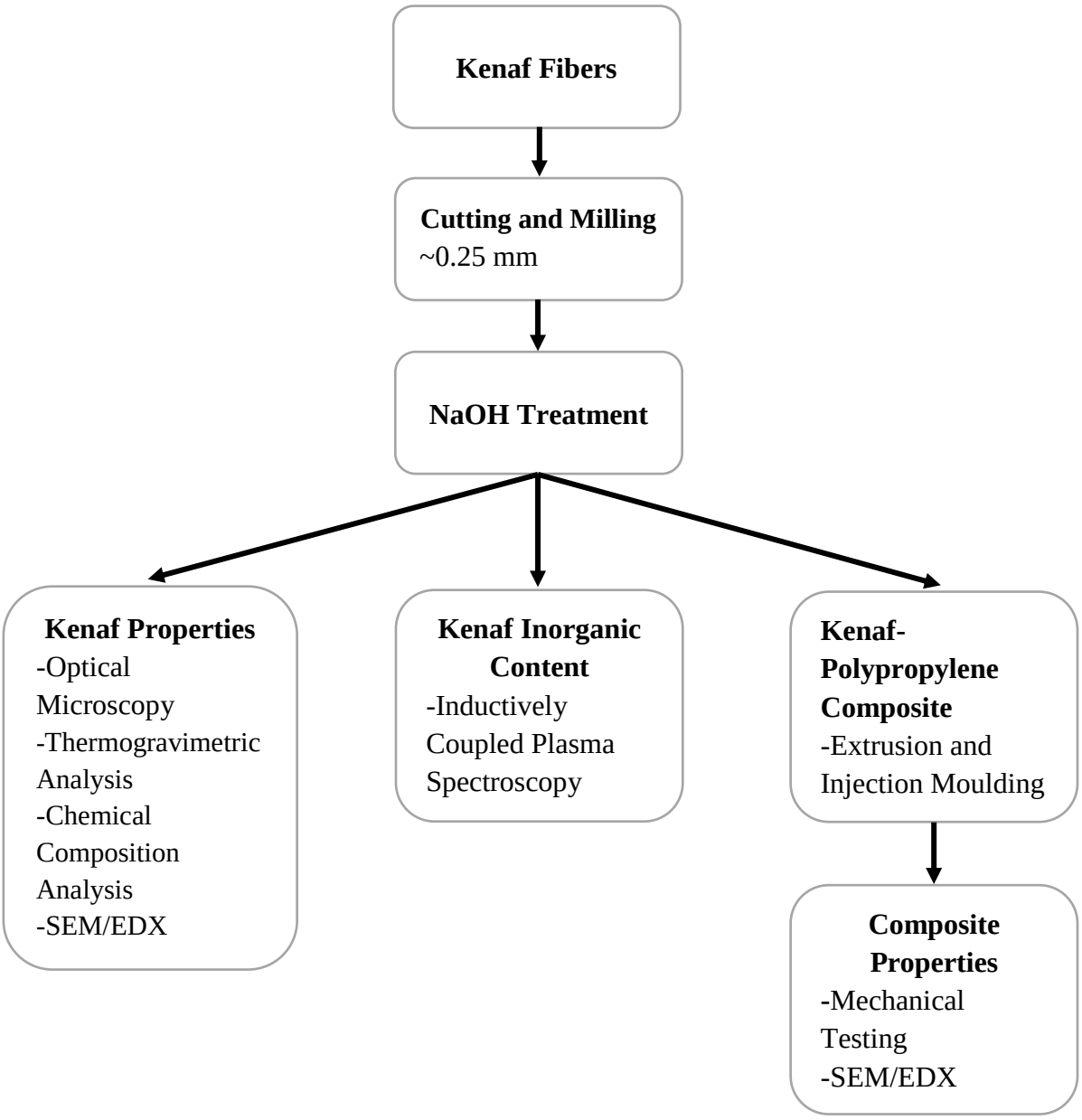

Figure 12: Overview of experimental procedure.

4.1 Materials

This section lists all chemicals, materials, equipment, and software used in this thesis as well as the associated supplier or manufacturer.

4.1.1 Chemicals

All chemicals and materials used in this thesis are shown in Table 12.

Table 12: Chemicals and materials with associated suppliers used in thesis.

Chemicals and Materials	Manufacturer	Location
DigiFILTER 0.45 micron	SCP Science	Canada
DigiTUBE Digestion Vessel	SCP Science	Canada
Glass Microfibre Filter, GF/B	Whatman	United Kingdom
Hydrochloric Acid (HCl), 37%	Sigma Aldrich	USA
Hydrofluoric Acid (HF), 49%	Fisher Scientific	USA
Kenaf Bast Fiber	Ontario Ministry of Agriculture, Food and Rural Affairs (OMAFRA)	Ontario, Canada
Liquid Nitrogen	Praxair	USA
Milli-Q Ultrapure Water	Millipore	USA
Nitric Acid (HNO_3), 70%	Sigma Aldrich	USA
Hydrion pH Papers	Micro Essential Lab	USA
Polypropylene Powder (PP), MFI 23-59	Goonvean Fibres	United Kingdom
Polypropylene Grafted Maleic Anhydride (MAPP), (8-10 wt.% maleic anhydride)	Sigma Aldrich	USA
Sodium Hydroxide (NaOH), solid	EMD Chemicals	USA

Kenaf fiber was provided by OMAFRA and was grown in Ontario, Canada, harvested in fall and then baled. The fibers were dried outside, dew retted, then stored indoors. Primary processing was done by decortication to separate the bast and core.

4.1.2 Equipment

All equipment used in the thesis are listed in Table 13.

Table 13: Equipment and associated suppliers used in thesis.

Equipment	Supplier	Location
4465 Testing Machine	Instron	USA
Axio Vert.A1-Inverted Microscope	Zeiss	Germany
Guillotine Paper Trimmer	Acme Westcott	USA
Desk II	Denton Vacuum	USA
Dyla Dual Hot Plate Stirrer	VWR	USA
Prodigy7 Inductively-Coupled Plasma Optical Emission Spectrometer	Teledyne Leeman Labs	USA
Quanta FEG 250 SEM, FEI	Thermo Fisher Scientific	USA
SJSZ-07A Micro-Compounder	Wuhan Ruiming	China
SQS-120 Pelletizing Machine	Wuhan Ruiming	China
SZS20 Injection Moulding Machine	Wuhan Ruiming	China
Thermolyne Type 2200 Hot Plate	Thermo Fisher Scientific	USA
Thermolyne Type F600 Furnace	Thermo Fisher Scientific	USA
TGA Q500	TA Instruments	USA
Ultra Centrifugal Mill ZM 200	Retsch	Germany
Vacuum Pressure Station	Barnant Company	USA

4.1.3 Software

All software used in this thesis are listed in Table 14.

Table 14: Software used in thesis.

Software	**Company**
Axio Vision	Zeiss
Bluehill Universal Software	Instron
Excel	Microsoft Corporation
ImageJ	National Institutes of Health and the Laboratory for Optical and Computational Instrumentation
INCA-Point & ID	Thermo Fisher Scientific
Jupyter	Jupyter
Python	Python
Salsa	Teledyne Leeman Labs
Universal Analysis 2000	TA Instruments-Waters LLC
Word	Microsoft
xT Microscope Control	Thermo Fisher Scientific

4.2 Preparation of Milled Kenaf Fiber

Firstly, kenaf fibers were cut with a guillotine paper trimmer (Acme Westcott, USA) to approximately 1cm lengths. The 1 cm long kenaf fibers were fed into an ultracentrifugal mill ZM 200 (Retsch, Germany), as shown in Figure 13, with a sieve with 0.25 mm trapezoid holes (part 03.647.0234) and a 6 teeth push-fit rotor (part 02.608.0040) to ensure fiber dust was smaller than 0.25 mm in at least one dimension. Kenaf fibers (1 cm long) were fed into the mill, 100 mL at a time. Once fibers were milled, MKF was removed and the process repeated until there was approximately 2 kg of MKF.

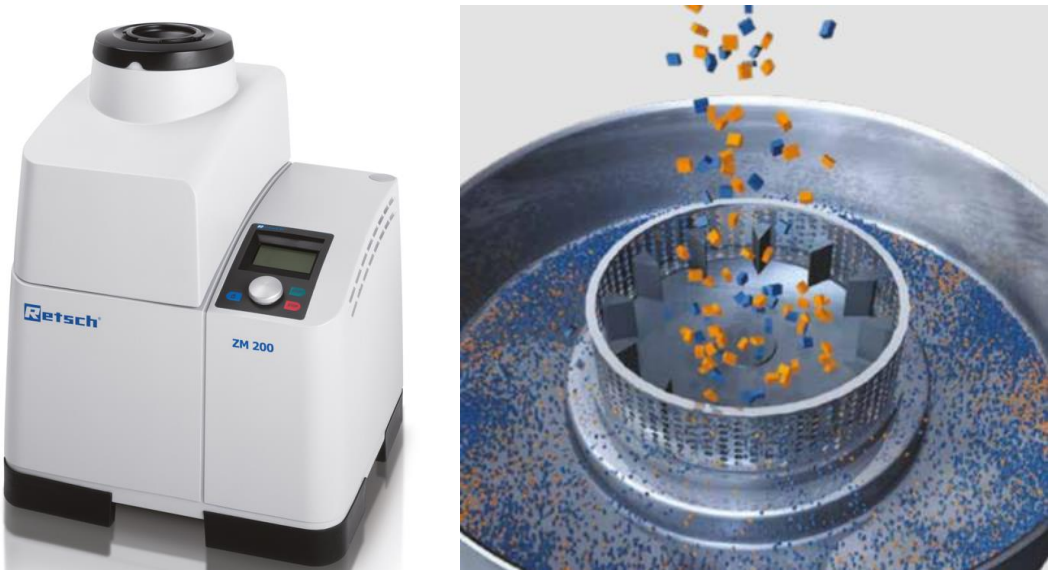

Figure 13: Retsch ZM 200 Ultracentrifugal Mill exterior and interior [90].

MKF was then mixed thoroughly in a large bin to ensure homogeneity and MKF was then stored until needed for further use.

4.3 Sodium Hydroxide (NaOH) Treatment

Sodium hydroxide was used to ret MKF with the objective of removing hemicellulose and other impurities to improve dispersion, and adhesion between kenaf and the polymer. MKF was treated with 0, 3 or 6 wt.% NaOH solution for two hours at either room temperature or 80°C while stirring (Table 15). The NaOH solution was prepared by dissolving NaOH pellets in milli Q water. NaOH treated MKF were made in 15 g batches in 500 mL of treatment solution in a 1000 mL beaker. Batches were stirred and heated (if necessary) with a Dyla Dual Hot Plate Stirrer (VWR, USA). The treated MKF was rinsed with milli Q water until a neutral pH was reached. pH was monitored with pH paper. The MKF was then filtered using glass microfiber filter papers (Whatman, United Kingdom) with a 1.0 µm pore size. Samples were left to air dry for 48 hours. Several batches of each MKF NaOH treatment were prepared to produce replicates as needed.

Table 15: NaOH treatment conditions and code.

Set Code	NaOH (%w/v)	Temperature (°C)
0-RT	0	Room Temperature
0-80	0	80
3-RT	3	Room Temperature
3-80	3	80
6-RT	6	Room Temperature
6-80	6	80

4.4 Optical Microscopy

Optical microscopy was used to visually assess MKF morphology with and without NaOH treatment. The samples of MKF were mounted on microscope slides and were observed using an Axio Vert.A1-inverted microscope (Zeiss, Germany). Fibers were viewed under 630 x magnification. Axio Vision software was used to capture images of MKF under magnification. Images were exported as PNG files and resized to fit this document.

Optical microscopy images magnified to 100x was analyzed for particle size using image analysis software (ImageJ). Fibers were measured using the “Straight” measuring tool in the software. 15 measurements were done for each fiber treatment.

4.5 Thermogravimetric Analysis

Thermogravimetric analysis (TGA) was used to assess the effect of the NaOH treatment on the thermal stability of MKF. MKF was prepared as described in Table 15. Thermogravimetric analysis was performed using thermogravimetric analyzer (TGA Q500, TA Instruments, USA). Approximately 20 mg of each sample was heated under nitrogen from 40°C to 600°C at 5°C/min. Data was processed in real time with Universal Analysis 2000 software and then data was exported in an Excel file. Data was then processed using Python code in Jupyter software to produce TGA and DTGA curves and to extract data on MKF composition.

4.6 Chemical Composition Analysis

Five grams of MFK, untreated and NaOH treated, samples were analyzed for acid detergent fiber (ADF), neutral detergent fiber (NDF), and lignin. The analysis was conducted by A&L Canada Laboratories Incorporated (London, Ontario) and was based on the ANKOM Technology A2000 method (acid detergent fiber method, neutral detergent fiber method, and acid detergent lignin method) using an ANKOM 2000 Fibre Analyzer. ADF corresponds to the residue after sulfuric acid and acetyl trimethylammonium bromide digestion. NDF corresponds to the residue after detergent solution digestion. The lignin determination was performed on remaining material after ADF determination. This was done by measuring the residue after further extraction with sulfuric acid. ADF represents the cellulose and lignin content of MKF while NDF represents cellulose, hemicellulose and lignin. The cellulose content was calculated by subtracting lignin content from ADF. The hemicellulose content was calculated by

subtracting ADF from NDF. Further information on the procedure used can be found at https://www.ankom.com/analytical-methods-support/fiber-analyzer-a2000.

4.7 Inductively Coupled Plasma Spectroscopy

Inductively coupled plasma optical emission spectroscopy (ICP-OES or ICP) was used for the analysis of the inorganic content of MKF. Prior to ICP analysis, MKF samples were dry-ashed and acid digested. Samples were dried in a Thermolyne F6000 muffle furnace (Thermo Fisher Scientific, USA) at 100°C until a constant weight was reached. The dried MKF was then dry-ashed at 575°C in the Thermolyne F6000 muffle furnace for 6 hours to produce kenaf ash. The kenaf ash was then digested in a DigiTUBE digestion vessel with a 2 mL mixture (1:2:28:20 volume ratio) of hydrofluoric acid (49%, Fisher Scientific, USA), hydrochloric acid (37%, Sigma Aldrich, USA), nitric acid (70%, Sigma Aldrich USA), and Milli Q water at 95°C for two hours on a Thermolyne Type 2200 Hot Plate (Thermo Fisher Scientific, USA). The digested ash solution was then filtered with DigiFILTER 0.45 micron (SPC Science, Canada) attached to a vacuum pressure station (Barnant Company, USA) in preparation for ICP. The filtered solution was diluted to a volume of 25 mL with Milli Q water. ICP analysis was performed on the digested samples for twenty elements (Mn, Fe, Cu, Ca, Zn, Na, Ni, Pb, Mg, K, Al, Ba, B, Cd, Cr, Co, Li, Sr, Si, and V). The analysis was conducted with a Prodigy7 Inductively Coupled Plasma Optical Emission Spectrometer (Teledyne Leeman Labs, USA) as shown in Figure 14.

Figure 14: Prodigy7 Inductively Coupled Plasma Optical Emission Spectrometer, Teledyne Leeman Labs.

Analysis was conducted in triplicate. The concentration was expressed in ppm of digested ash solution by Salsa software. The data was exported as an Excel file and was converted to µg kenaf/g fiber using Microsoft Excel. A sample calculation of the conversion from ppm to µg kenaf/g fiber is shown in equation (3).

$$5\ ppm\ Mn = \frac{5\ \mu g\ Mn}{g\ solution}$$

$$\frac{5\ \mu g\ Mn}{g\ solution} \times \frac{1\ g\ solution}{mL\ solution} \times \frac{25\ mL\ solution}{5\ g\ MKF} = 25\ \frac{\mu g\ Mn}{g\ MKF} \quad (3)$$

4.8 Composite Preparation

This section gives the methodology for the preparation of MKF-polypropylene composite materials. Three sets of composites were prepared using a common methodology. The purpose of the first set was to identify the maximum MKF content. The purpose of the second set was to asses the effect of polypropylene grafted maleic anhydride (MAPP) content. The purpose of the third set was to investigate the effect of NaOH treatment for constant MKF content (30 wt.%) and the effect of MAPP.

4.8.1 Material Composition

The first set of composites was prepared using untreated MKF and polypropylene (PP). The composition of each composite of the first set is summarized in Table 16.

Table 16: Composition of the first set of MKF-PP composites to assess maximum MKF.

Code	MKF (% w/w)	PP (% w/w)
PP	0	100
20MKF-80PP	20	80
30MKF-70PP	30	70
40MKF-60PP	40	60

The second set of composites was prepared using untreated MKF, PP and MAPP. Two different compositions were prepared. The first composition had 20 wt.% MKF, 77 wt.% PP, and 3 wt.% MAPP (20MKF-77PP-3M). The second composition had 30 wt.% MKF, 67 wt.% PP, and 3 wt.% MAPP (30MKF-67PP-3M).

The third set of composites were made with NaOH treated MKF from Table 15, PP and MAPP. The composition of each composite is summarized in Table 17.

Table 17: Composition of the third set of composites to assess effect of NaOH treatment.

				MKF Treatment	
Code	**PP (% w/w)**	**MKF (% w/w)**	**MAPP (% w/w)**	**NaOH (% w/v)**	**Temp. (°C)**
PP	100	0	0	0	N/A
0-RT	70	30	0	0	RT
6-RT	70	30	0	6	RT
0-80	70	30	0	0	80
6-80	70	30	0	6	80
0-RT-M	67	30	3	0	RT
6-RT-M	67	30	3	6	RT
0-80 M	67	30	3	0	80
6-80-M	67	30	3	6	80

Room temperature is represented by RT.

4.8.2 Extrusion

MKF, powdered PP and MAPP (if present) were manually mixed according to the design ratio in 7 g batches for each sample of each set. The mixed MKF, PP and MAPP (if present) were fed into a counter-rotating twin screw micro-compounder (SJSZ-07A, Wuhan Ruiming, China) as shown in Figure 15. The MKF, PP and MAPP were mixed in the counter-rotating twin screw micro-compounder for 5 minutes before extrusion. The screw speed was 24 rpm and was

divided into four temperature zones. The temperatures were 165°C, 170°C, 175°C, and 185°C from the hopper to the die.

Figure 15: Wuhan Ruiming Twin-Screw Micro-Compounder.

4.8.2.1 Injection Moulding

Once the material was extruded into a filament, the filament was cut into pellets using pelletizing machine (SQS-120, Wuhan Ruiming, China). The pellets were then fed to the injection moulding machine (SZS20, Wuhan Ruiming, China). The injection zone was set to 200°C and approximately 0.7 MPa of pressure while the molding board zone was set to 65°C and

approximately 0.3 MPa to produce bars. The dimensions of the “dog bone” bars were 2 mm in thickness, 75 mm in overall length, 10 mm for overall width, and 5 mm in narrow width according to ASTM-D638 as shown in Figure 16 [91]. Samples were stored at room temperature until needed for further tests.

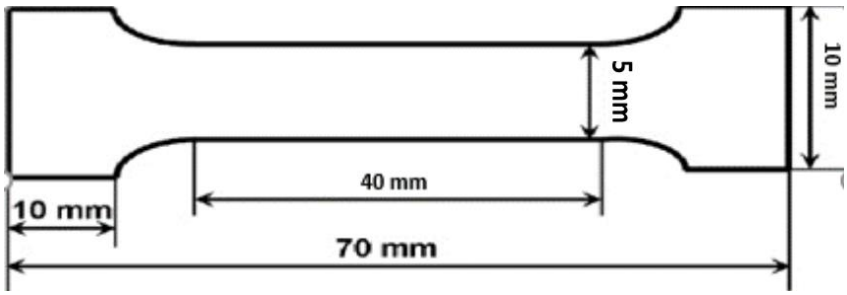

Figure 16: Tensile test specimen dimension.

4.9 Mechanical Properties

The tensile strength, Young’s modulus, and elongation at break were determined in accordance with ASTM-D638 [91]. Samples were evaluated with an Instron Testing Machine (4465, Instron, USA), as shown in Figure 17, at a rate of 5 mm/min. In set 1 and 2, three samples were used for each type of composite while in set 3, seven samples were used for each type of composite. The data was exported by Bluehill Universal Software as an Excel file and was processed in Python code using Jupyter and Excel. Set 3 data is plotted as a mean ± standard deviation, n=7.

Figure 17: Instron Testing Machine.

4.10 Scanning Electron Microscopy and Energy Dispersive X-Ray Spectroscopy

Scanning electron microscopy (SEM) was used to observe the surface of MKF morphology and the fractured composite cross-section. Composite bars were fractured after immersion in liquid nitrogen. Samples were then coated with gold in argon with the gold coating unit Desk II (Denton Vacuum, USA). Coated samples were observed with a Quanta FEG 250 SEM (Thermo Fisher Scientific, USA) at an electron voltage at 20 kV. The Quanta FEG 250 SEM was used to perform SEM and EDX analysis. SEM images with sample surfaces relatively

perpendicular to the direction of the electron beam were chosen. SEM images were processed with xT Microscope Control software which exported images as a TIF file. MKF was viewed 500-2000x magnification. Composite bar cross-sections were viewed 500-5000x magnification.

EDX was processed with INCA-Point & ID software which exported data in Microsoft Word. EDX was performed at 500 x magnification for MKF and 1000 x magnification for composite bar cross-sections.

4.11 Statistical Analysis

Statistical analysis was performed with a combination of Microsoft Excel and Python in Jupyter. Analysis of variance (ANOVA) with a 90% confidence interval was performed on ICP data of MKF and mechanical properties of composites to assess the effects of the treatments.

5 Results and Discussion

Firstly, the effect of sodium hydroxide on the treatment of milled kenaf fiber (MKF) will be presented, namely, the effects on structure, thermal stability and inorganic content. Secondly, the effect of sodium hydroxide treatment on milled kenaf fiber-polypropylene composite performance will be discussed in terms of morphology and mechanical properties.

5.1 Kenaf Milling

Kenaf as received was tangled (Figure 18). Kenaf was milled into MKF as shown in Figure 19.

Figure 18: Kenaf fiber as received. Ruler for scale (in cm).

Figure 19: Milled kenaf fibers. Ruler for scale (in cm).

5.2 Optical Microscopy

Optical microscopy was performed to assess kenaf surface protrusions and formation of microfibrils as well as MKF size.

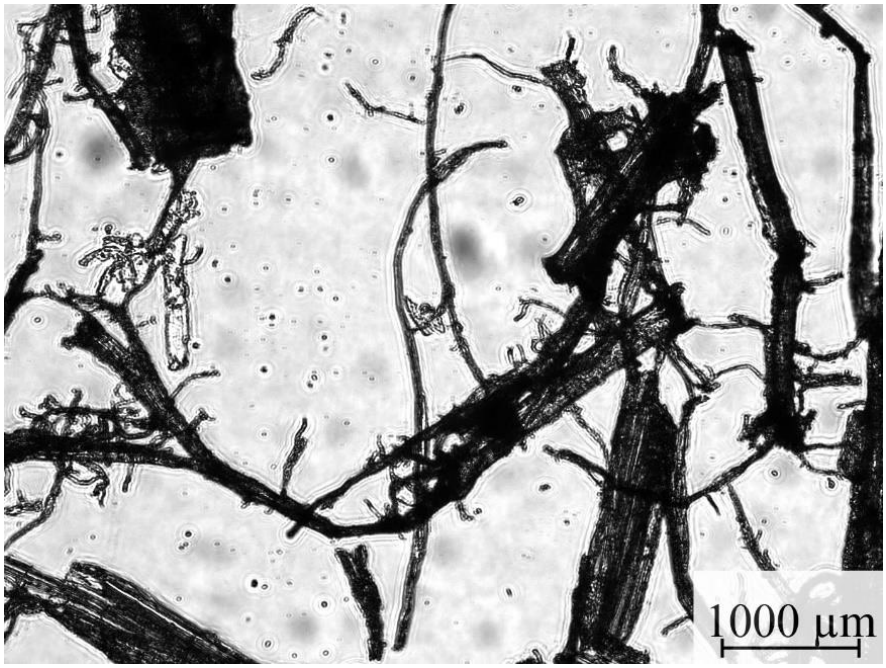

Figure 20: Optical microscopy images of 6-80 MKF under lower magnification (100x).

Figure 20 highlights the large variations in the morphology of fiber after alkalization with 6% NaOH at 80°C. It is difficult to compare fiber diameters between treatments because of this variation. Both small fibrils and large fiber bundles can be seen.

The particle length distribution, shown Figure 21 and Figure 22, indicates 75.6% of fiber lengths are shorter than 500 µm while 16.7% of fiber are between 500 and 1000 µm. 1.1% of fibers were between 2000-2500 µm, 3500-4000 µm, and 4000-45000 µm, respectively. When comparing fibers treated at room temperature and 80°C fiber size distribution is similar. When comparing fibers based on NaOH concentration, fiber lengths are longest for MKF treated with 0% NaOH, followed by 3% NaOH. Increasing NaOH concentration decreased fiber length.

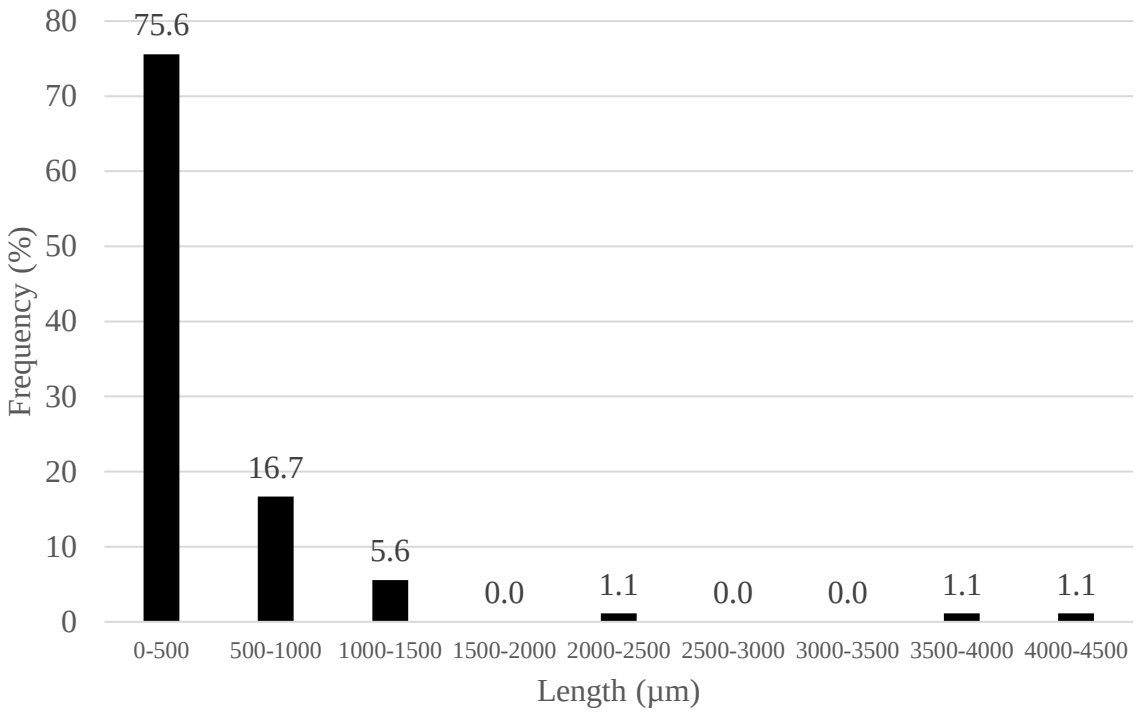

Figure 21: Fiber length distribution for MKF with various alkali treatment (0%, 3%, and 6% NaOH at room temperature and 80°C).

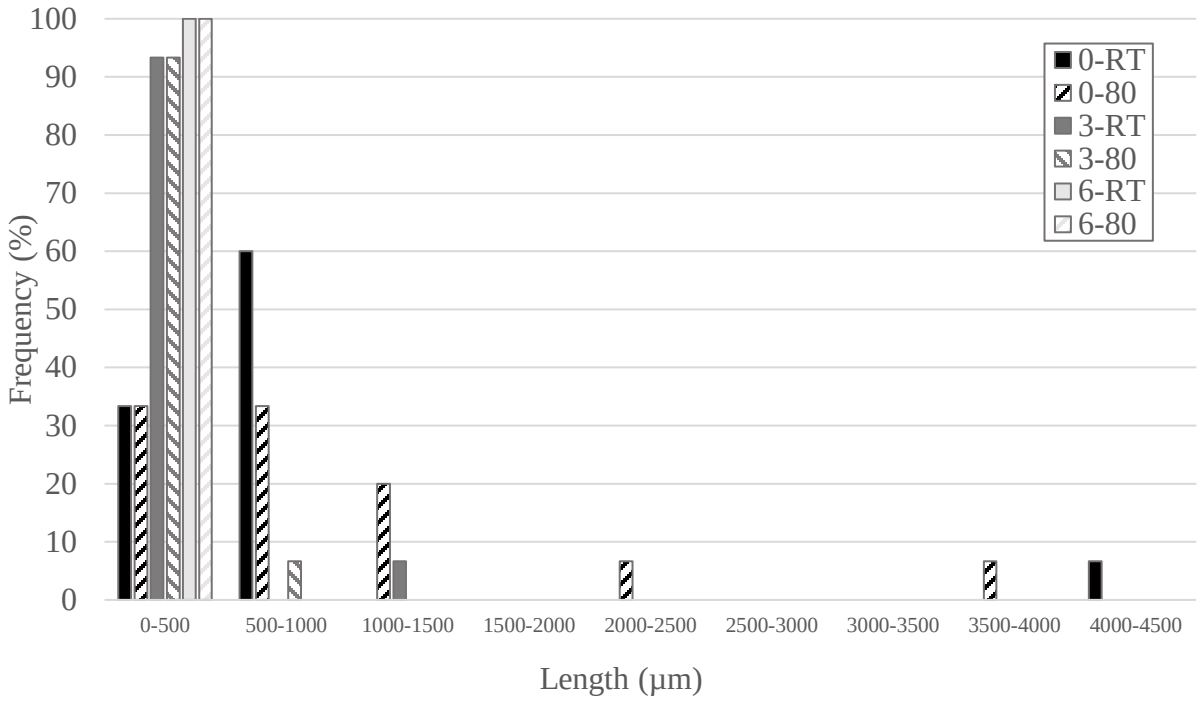

Figure 22: Length distribution of MKF with varying NaOH treatment.

Thin protrusions may be observed by focusing on the shape of the outline of fibers using optical microscopy. Thin protrusions observed forming off the main fiber bundle are indicative of fibrillation. Images which best represent general features of the samples were chosen and are presented in Figure 23.

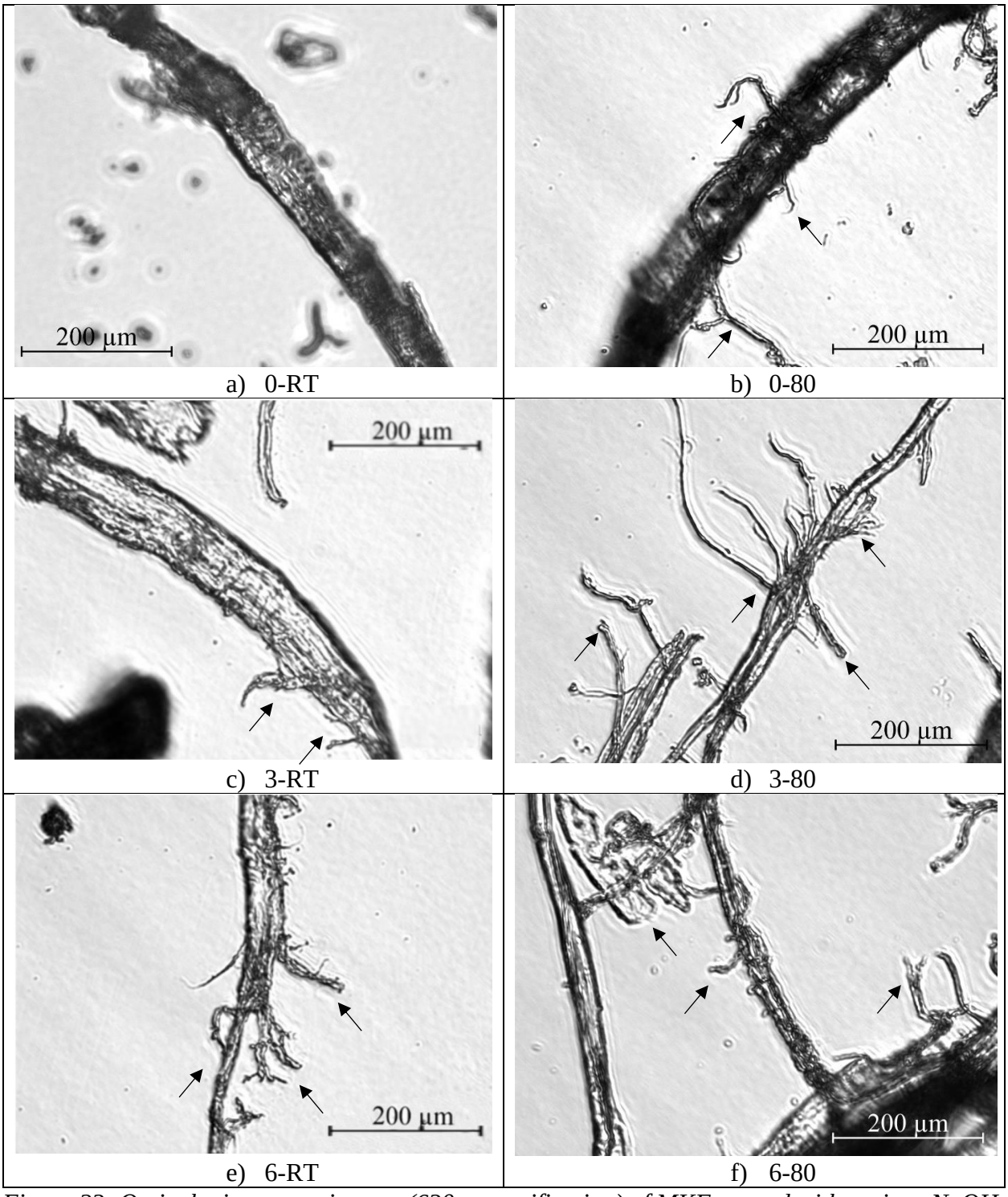

Figure 23: Optical microscopy images (630x magnification) of MKF treated with various NaOH solutions. Arrows indicate thin protrusions on the surface. a) 0-RT: water at room temperature, b)0-80: water at 80°C, c) 3-RT: 3% NaOH at room temperature, d) 3-80: 3% NaOH at 80°C, e) 6-RT: 6% NaOH at room temperature, f) 6-80: 6% NaOH at 80°C.

When comparing fiber based on temperature changes, that is from room temperature to 80°C, no effect could be identified. At 0% NaOH, there is increased fibrillation and thin protrusions which is indicated by black arrows in Figure 23 b). At 3% NaOH, there is also an increase in thin protrusions and the formation of more microfibrils at 80°C when compared to room temperature. At 6% NaOH, there is no noticeable difference in microfibril formation. The increase in temperature from room temperature to 80°C improves effects from NaOH treatments for lower concentrations (0% and 3% NaOH) but does not show improvement at 6% NaOH.

It is expected that higher temperatures would increase the effect of the NaOH treatment. When compared to room temperature, kenaf fibers treated at 95°C with 6% NaOH are expected to improve the tensile performance of a composite [56]. When comparing images of room temperature and 80°C NaOH treated MKF, effects from treatments were more pronounced for 0% and 3% NaOH but not for 6% NaOH. Increased fibrillation may be caused by NaOH or by fiber swelling from water in the solution. The 6% NaOH treatments may not show a difference between room temperature and heated samples because the effect from the alkali solution greatly outweighs noticeable effects from heating the fiber. It should be noted that the temperature used in this study is not as high as some reported temperatures nor is it treated as long. Edeerozey et al. found that 6% NaOH treatment at 95°C for three hours produced kenaf with the highest unit break [56].

At room temperature, the effect of NaOH concentration can be compared. As the concentration of NaOH increases, so does the fibrillation of the fiber. This is indicated by black arrows in Figure 23 c) and e). At 80°C there is increased fibrillation from 0% to 3% NaOH

treatments. However, 3 and 6% NaOH treatments do not show noticeable differences in fibrillation.

Thin protrusions on the surface are expected to increase with NaOH concentration as NaOH removes hemicellulose, and lignin from MKF to expose cellulose microfibrils. NaOH will react with hydroxyl groups on the fiber breaking down the fiber and causing fibrils to move outwards. Optimal alkalization conditions may occur at 6% NaOH as suggested by Edeerozey's tensile tests [56]. It is therefore expected that fibrillation will increase with temperature and increase as the concentration of NaOH approaches 6%. This is noticed for room temperature treated samples with NaOH concentrations increasing from 0% to 3% and finally 6%. The trend of increasing protrusions and fibrillation is also seen at 80°C between 0% and 3% but not between 3% and 6% NaOH. It was not possible to distinguish if treatment 6-80 was superior to either a lower concentration (3-80) or a lower temperature (6-RT).

5.3 Thermogravimetric Analysis

Thermogravimetric analysis (TGA) was used to assess the effect of the sodium hydroxide treatment on the composition of milled kenaf fiber. Kenaf fiber contains three major organic constituents (cellulose, hemicellulose and lignin) each with distinct thermal stability. The expected degradation temperatures are 315-400°C for untreated cellulose, and 220-315°C for untreated hemicellulose. Untreated lignin is expected to degrade across the temperature range (40-600°C) presented [73]. There is also mass loss expected at temperatures below 100°C from the removal of water.

Figure 24, Figure 25, and Table 18 summarize the TGA analysis. When comparing the temperature of the 3 and 6% NaOH treatment, an increase in treatment temperature led to a decrease in thermal resistance as indicated by mass loss occurring at lower temperatures. This may be due to conformational and chemical changes in cellulose. With 0% NaOH treatment this leftward shift is not seen in samples treated at 80°C. The DTG curve shows that 0-RT had a higher moisture content than 0-80. The MKF treated at 80°C had higher $T_{5\% \text{ onset}}$ than MKF treated at room temperature. This may be due to the removal of thermally unstable compounds in the treatment step at 80°C.

In MKF treated with 0% NaOH, there was a decrease in T_{max} and an increase in final residual mass. The opposite was observed for MKF treated with 3 and 6% NaOH. At 3 and 6% NaOH, an increase in treatment temperature resulted in a higher T_{max} and a lower residual mass. There may be interactions between NaOH and temperature that explain the differences in the T_{max} and residual mass. When combined with NaOH, an elevated temperature increased the thermal stability of the MKF but may have removed mineral content in the residual mass.

At room temperature, the effect of NaOH concentration may be obtained from TGA analysis. The $T_{5\% \text{ onset}}$ is lowest for 0-RT due to the large moisture content in its original mass. The $T_{5\% \text{ onset}}$ is highest in 3-RT followed by 6-RT. The T_{max} was highest for 0-RT followed by 6-RT and finally 3-RT. This suggests that cellulose was most thermally stable at 0-RT. The residual mass at 600°C was the same for 3-RT and 6-RT and was the lowest for 0-RT. This may be due to 0-RT having a greater proportion of hemicellulose by mass that was removed in 3-RT and 6-RT treatments.

DTG peaks for the treatments at 3% NaOH, are very similar to the corresponding peaks after 6% NaOH treatment. When comparing the DTG curves of 0-RT, 3-RT, and 6-RT, there is a change in shape. 0-RT has a shoulder in the curve from approximately 240°C to 325°C which corresponds with the degradation of hemicellulose. This shoulder is not visible in 3-RT and 6-RT suggesting that hemicellulose was removed with these NaOH treatment. The 0-RT MKF also had the most moisture content as shown by the peak at the beginning of the 0-RT run (40-90°C). The major peak in the DTG curves shows the presence of cellulose between 325°C and 400°C. This aligns with temperatures for purified cellulose decomposition (315-400°C) [73] as well as the cellulose peak from untreated flax fibers (340-370°C) [75]. However, the cellulose peak from water treated kenaf was lower (270-330°C) than was reported in this study [74].

At 80°C, the effect of NaOH was analyzed. A similar trend is seen at 80°C for $T_{5\% \text{ onset}}$ as was seen at room temperature. $T_{5\% \text{ onset}}$ is lowest at 0-80, followed by 6-80 and the highest value is at 3-80. The T_{max} decreased with increasing NaOH concentration. The residual mass is lowest for 0-80, followed by 6-80, and 3-80 has the highest value for residual mass. The low residual mass of 0-RT may be related to the larger proportion of thermally unstable fiber hemicellulose.

There is a shoulder in 0-80 between 240°C and 325°C which corresponds to hemicellulose which is not present in 3-80 or 6-80. This implies that there is removal of some hemicellulose with these NaOH treatments. Moisture content varied by less than 1% between treatments with 0-RT having the largest moisture content (4.9 wt.%). Similarly to treatments done at room temperature, there were cellulose peaks present for 0-80, 3-80, and 6-80 between 325°C and 400°C which aligns with literature values for cellulose (315-400°) [73].

It was found that the hemicellulose peak and cellulose peak overlap. Efforts were made to deconvolute the peaks to determine quantitative results for hemicellulose and cellulose removal. In Python, non-linear least squares was used to fit a Gaussian model and Lorentzian model in an attempt to deconvolute the peaks. However, the fit was poor as the peaks were found to overlap too closely. Therefore, deconvolution attempts are shown only in the appendix.

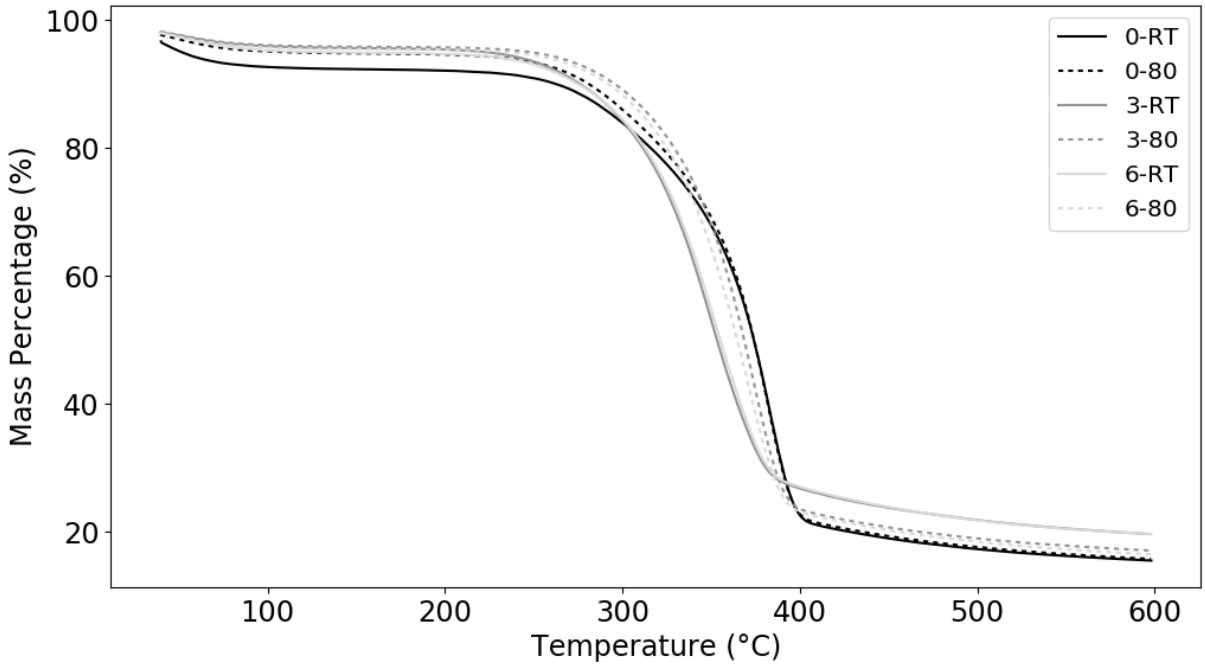

Figure 24: TGA curve of MKF according to NaOH treatment under nitrogen at 5°C/min.

(a)

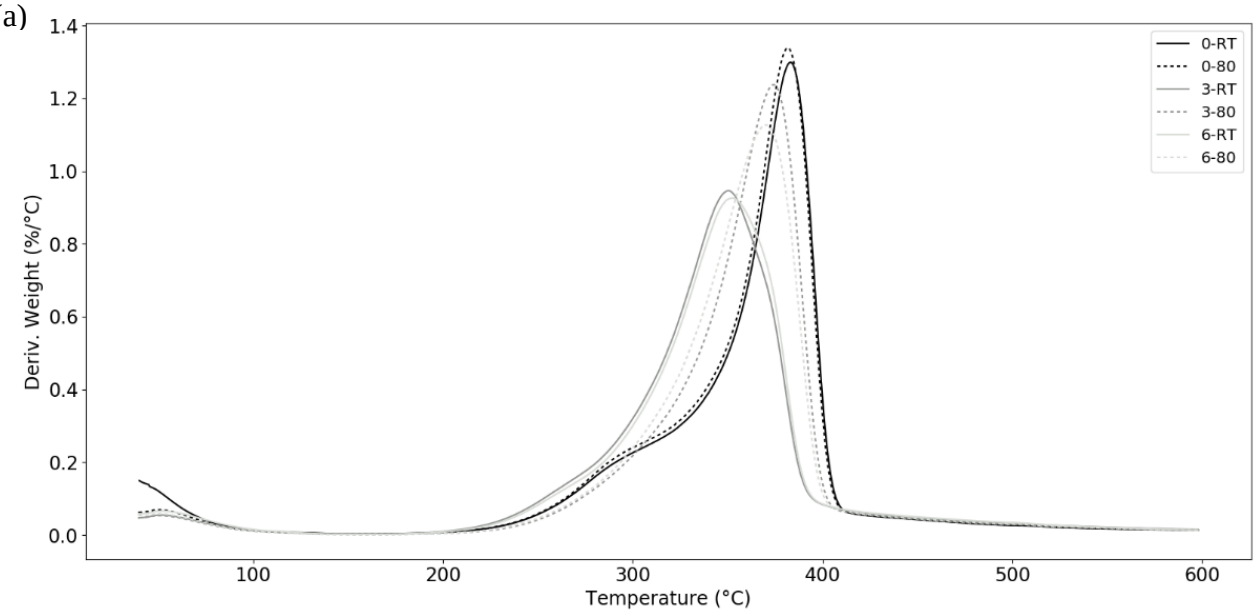

(b)

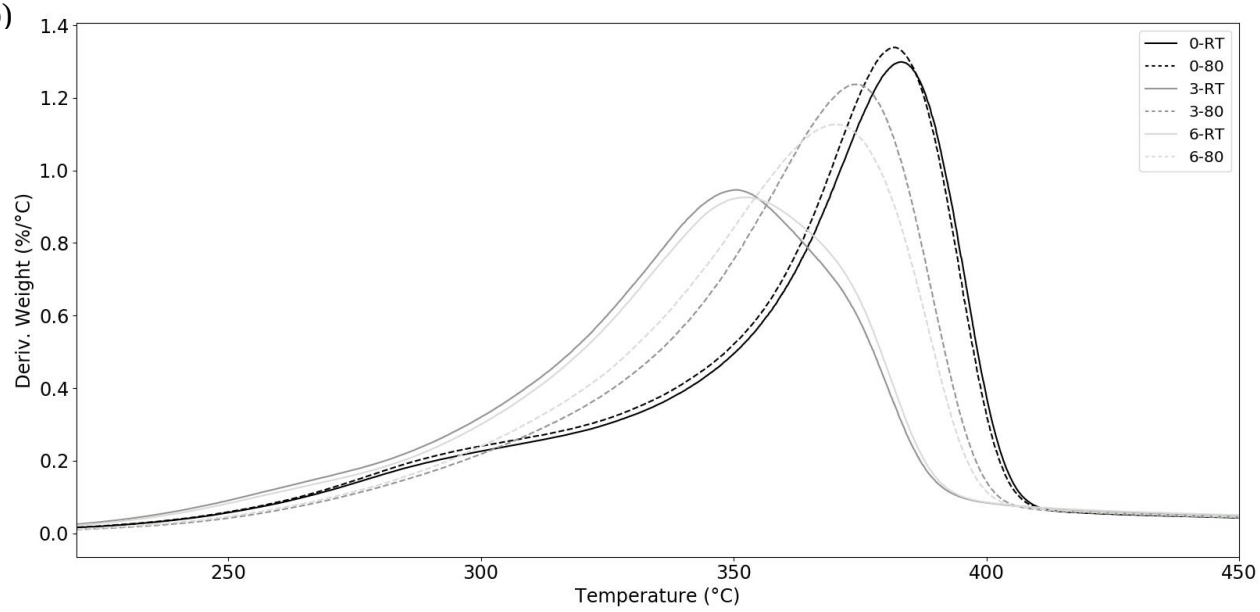

Figure 25: DTG curves of MKF according to NaOH treatment under nitrogen at 5°C/min. (a) 40-600°C (b)220-450°C.

Table 18: Thermal behaviour of MKF with NaOH treatment.

Code	$T_{5\% onset}$ (°C)	T_{max} (°C)	Residual Mass at 600°C (wt. %)
0-RT	51.1	383.1	15.5
0-80	105.8	381.8	15.7
3-RT	221.2	350.6	19.6
3-80	246.5	374.1	17.0
6-RT	119.8	352.2	19.6
6-80	233.0	370.1	16.4

The TGA analysis in conjunction with optical microscopy images show that some retting took place and that some hemicellulose was removed. With the removal of hemicellulose, cellulose fibrils would therefore be exposed to give increased fibrillation. At both 3% and 6% NaOH treatments some retting occurred. Some hemicellulose was removed, and, from that aspect, retting was successful at both NaOH concentrations. It is important to recognize the point at which the removal of hemicellulose occurs as it is an indicator of successful retting. Prolonged NaOH treatment of kenaf may lead to poor performance in composite.

5.4 Chemical Composition

Table 19 shows results from composition analysis showing mass fraction of cellulose, hemicellulose, and lignin. Statistical analysis was not performed on samples as there were no replicates performed. The cellulose content of untreated MKF is lowest when compared to all other treated MKF. In contrast, the hemicellulose and lignin content of the untreated MKF is similar to the 0-RT MKF but different compared to all other treated MKF.

MKF treatment temperature may also be compared. At 0% NaOH, samples with a higher treatment temperature (80°C) showed similar values for cellulose and lignin, and 12% more hemicellulose than MKF treated at room temperature. MKF treated with 3% NaOH show 8% more cellulose, 11% less hemicellulose and 13% less lignin at 80°C treatment temperature when compared to room temperature. MKF treated with 6% NaOH show 2% more cellulose, 6% less hemicellulose, and 2% more lignin at 80°C treatment temperature when compared to room temperature. This shows that there is some removal of hemicellulose associated with a higher treatment temperature in the presence of NaOH. However, the relationship between cellulose and lignin, and temperature is unclear.

There can also be comparison made base on NaOH concentration. At room temperature increasing NaOH concentration from 0% to 3% (0-RT to 3-RT) results in a 6% increase in cellulose. Increasing NaOH concentration from 3% to 6% (3-RT to 6-RT) results in similar cellulose mass fraction with a 1% increase in cellulose. Increasing NaOH concentration from 0% to 3% NaOH (0-RT to 3-RT) results in 20% lower hemicellulose mass fraction but 35% higher lignin mass fraction. Increasing NaOH concentration from 3% to 6% NaOH (3-RT to 6-RT)

results in a 10% increase in the mass fraction of hemicellulose but 19% lower mass fractions of lignin. The data shows that NaOH treatment at room temperature increases cellulose extraction but the relationship between NaOH concentration, and hemicellulose and lignin is unclear.

At 80°C, increasing NaOH concentration from 0% to 3% NaOH (0-80 to 3-80) results in 15% higher mass fraction of cellulose, 37% lower mass fraction of hemicellulose, and 19% higher mass fraction of lignin. Increasing the concentration from 3% to 6% NaOH (3-80 to 6-80) results in 5% lower mass fraction of cellulose, 16% higher mass fraction of hemicellulose and 11% higher mass fraction of lignin. This shows that there may be effects from the interaction between NaOH concentration and treatment temperature. Overall, NaOH treatments used increase mass fraction of cellulose, while decreasing hemicellulose which agrees with data obtained from TGA (5.3).

Literature values show that untreated kenaf typically has 31-57 wt.% cellulose, 21.5-23 wt.%, hemicellulose and 8-19 wt.% lignin [2]–[5]. Compared to literature values, MKF from this study has high cellulose content (at least 11% greater), low hemicellulose content (at least 40% less), and similar lignin content. From literature, it is seen that NaOH treatment can remove between 28-84 wt.% of the total hemicellulose in kenaf, hemp and flax with 5-18% NaOH treatments [33], [52], [53]. It is therefore expected that there is 28-84 wt.% hemicellulose removed from kenaf in this thesis. However, hemicellulose removal ranged between 12-37%.

Table 19: Cellulose, hemicellulose and lignin content of MKF according to NaOH treatment. n=1.

Code	Cellulose (wt. %)	Hemicellulose (wt. %)	Lignin (wt. %)
untreated	63.43	11.38	10.00
0-RT	68.73	11.51	9.93
0-80	68.11	12.94	9.73
3-RT	72.68	9.24	13.37
3-80	78.65	8.19	11.62
6-RT	73.25	10.16	10.87
6-80	74.62	9.53	12.87

5.5 Inductively Coupled Plasma Spectroscopy

Inductively coupled plasma spectroscopy (ICP) analysis was done to quantify the inorganic content in MKF when treated with NaOH solutions. Elemental analysis of the ash obtained from MKF is shown in Table 20 and Figure 26.

Table 20: ICP elemental analysis of ash obtained from MKF according to sodium hydroxide treatment.

	Elemental Composition (μg element/g fiber) (avg ± SD, n=3)					
Treatment / Element	**0-RT**	**0-80**	**3-RT**	**3-80**	**6-RT**	**6-80**
Major Elements						
Ca	4752.4 ±74.9	4503.2 ±231.2	4907.5 ±310.9	4981.7 ±251.3	4421.8 ±88.5	4521.8 ±175.9
Si	3292.5 ±154.1	3020.9 ±210.5	2961.5 ±275.8	3901.6 ±880	3596.5 ±414.9	3924.6 ±333
Mg	989.5±983.7	791.3±695.8	428±25.3	749.1±463.6	421.7±55.4	475.8±13.1
Al	861.9±33.6	855.5±28.3	708.1±13.3	837.5±96.3	689.7±97.1	743±16.6
Fe	504.9±29.8	488.8±18.7	420.8±15.9	469.6±54.7	399.3±57.9	435.9±14.5
Na	323.5±40.7	271.5±12.7	1792.9 ±45.7	1222.7 ±123.1	1651.8 ±11.9	884.5 ±75.6
K	279.6±26.7	299.5±42.2	191.3±5.6	236±23.5	170.1±32.7	210.1±5.6
B	144.7±264.8	383.9±53.9	632.6±74.5	682.7±15.7	401.2±40.9	209.6±83.8
Minor Elements						
Ni	123.4±59.9	56.8±4.3	53.0±4.0	50.9±6.2	35.4±5.1	35.1±1.1
Mn	52.1±1.5	48.3±2.8	51.2±8.6	51.6±3.9	43.9±5.8	49.8±1.2
Ba	39.9±1.7	22.2±0.4	64.9±2.1	41.5±4.6	27.6±4.6	21±1.3
Zn	29.0±10.8	13.1±7.3	46.9±12.6	24.1±5.1	13.9±2.2	11.7±1.9
Pb	15.8±26.9	-1.3±1.2	-3.3±0.5	17±31.3	3.2±2.5	0.2±2.8
Sr	13.5±0.6	13.2±0.6	15.1±2.9	14.5±1.6	13.3±1.7	10.8±0.3
Cr	6.4±0.2	4.1±0.9	8.9±0.4	8.2±1.7	8.0±0.5	7.9±1.1
Y	4.2±7.2	-0.2±1.2	1.8±5.4	1.9±6.1	11.1±17.4	4.9±4.8
Cu	4.1±1.2	4.0±2.1	2.4±1.3	1.7±0.8	0.8±0.4	1.2±1.9
Co	0.4±0.4	0.2±0.1	0.4±1.8	0.4±0.2	0.0±0.7	0.4±0.5
Cd	0.4±0.5	1.1±0.2	3.2±4.6	-0.4±0.9	0.3±0.4	0.1±1.3
Li	0.2±0.7	0.4±0.4	5.7±9.5	0.4±0.8	1.1±0.3	0.9±0.4
V	-0.9±3.4	-1.5±2.3	-2.0±0.4	-1.5±1.9	-1.7±0.4	-2.2±0.1

Note that the silicon estimate may not represent only the content of the MKF. Some silicon from the glassware may have dissolved in the HF treatment resulting in a higher silicon content than expected in the MKF ash. Table 21 shows all the elements (excluding silicon) expressed as a wt. % of the MKF. The inorganic content measured by ICP is two orders of magnitude lower than the residual mass at 600°C (Table 18). This suggests that the residual mass estimated by TGA contains other constituents.

Table 21: Total inorganic element content.

Code	Total Inorganic Element (wt. % element/fiber)
0-RT	0.81
0-80	0.78
3-RT	0.93
3-80	0.94
6-RT	0.83
6-80	0.76

Total includes all elements from ICP analysis except silicon.

Seven elements with concentrations greater than 150 µg element/g fiber but excluding silicon (Fe, Ca, Na, Mg, K, Al, and B) are shown in Figure 26. These elements have been

reported to depend on growing conditions [92]. Calcium was the most plentiful of the elements tested (>4421.8 µg/g).

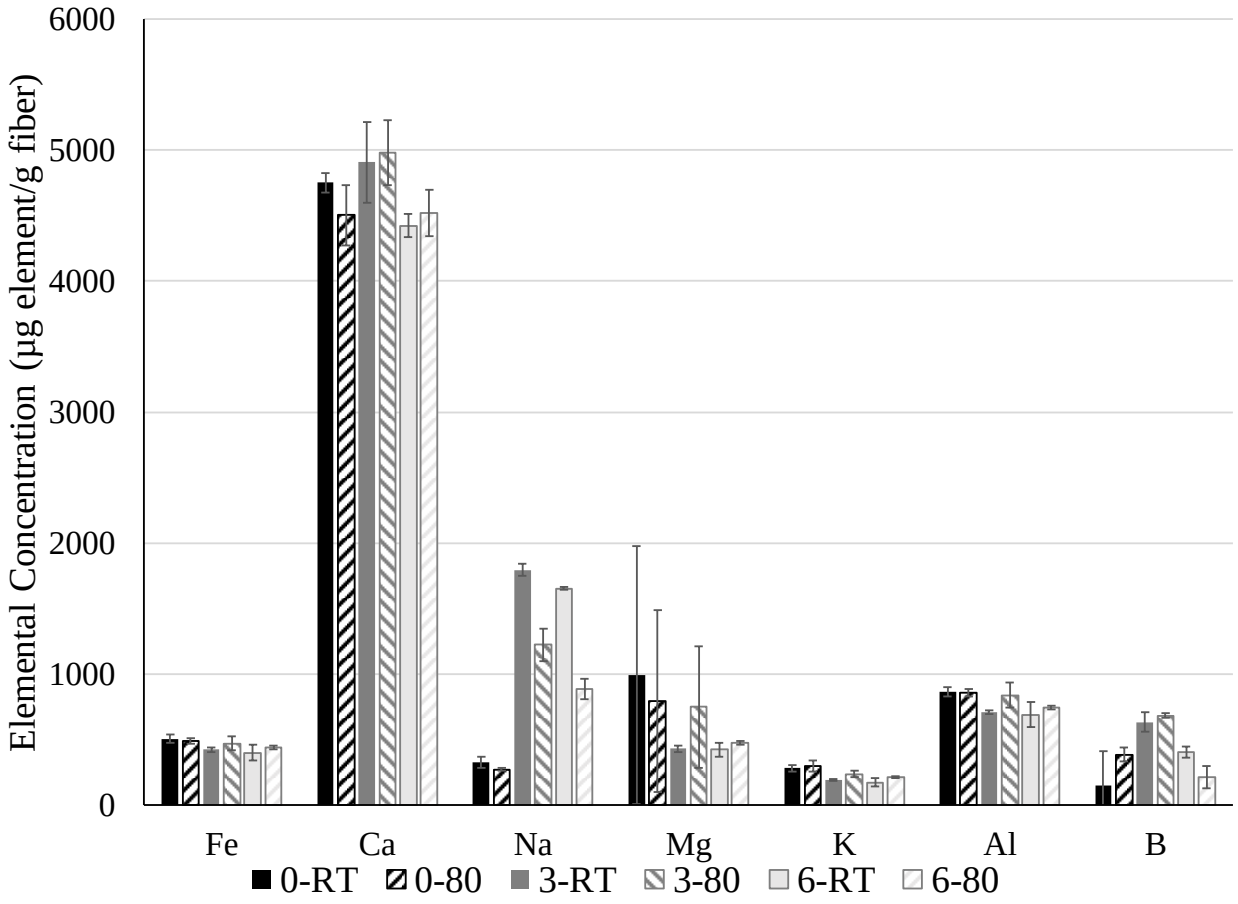

Figure 26: Elemental analysis of ash obtained from MKF according to NaOH treatment for content greater than 150 µg element/g fiber. Error bar shows standard deviation from average values (n=3).

ANOVA analysis (90% confidence interval) of the effect of NaOH treatments for each major element was performed using Excel and is shown in Table 22 to Table 28. ANOVA analysis is summarized in Table 29.

Table 22: ANOVA analysis of Fe content of MKF with NaOH treatment.

Source	SS	df	MS	F_{obs}
[NaOH]	19405.1835	2	9702.592	7.23583*
Temperature	2405.53759	1	2405.538	1.79396
Interaction	19651.9226	2	9825.961	7.32783*
Error	16090.9106	12	1340.909	
Total	41462.6436	17	2438.979	
	$F_{1,12,0.10}$=3.17655	**$F_{2,12,0.10}$=2.8068**	**$F_{5,12,0.10}$=2.39402**	

* indicates a significant effect.

Table 23: ANOVA analysis of Ca content of MKF with NaOH treatment.

Source	SS	df	MS	F_{obs}
[NaOH]	696565.3	2	348282.6	8.11196*
Temperature	2808.86	1	2808.86	0.06542
Interaction	628796.8	2	314398.4	7.32275*
Error	515213.7	12	42934.47	
Total	1328171	17	78127.7	
	$F_{1,12,0.10}$=3.17655	**$F_{2,12,0.10}$=2.8068**	**$F_{5,12,0.10}$=2.39402**	

* indicates a significant effect.

Table 24: ANOVA analysis of Na content of MKF with NaOH treatment.

Source	SS	df	MS	F_{obs}
[NaOH]	4929236	2	2464618	593.3445*
Temperature	965225.5	1	965225.5	232.3732*
Interaction	459286.5	2	229643.3	55.2855*
Error	49845.27	12	4153.772	
Total	6353748	17	373749.9	
	$F_{1,12,0.10}$=3.17655	**$F_{2,12,0.10}$=2.8068**	**$F_{5,12,0.10}$=2.39402**	

* indicates a significant effect.

Table 25: ANOVA analysis of Mg content of MKF with NaOH treatment.

Source	SS	df	MS	F_{obs}
[NaOH]	611397.7	2	305698.8	1.09793
Temperature	15651.14	1	15651.14	0.05621
Interaction	3543521	2	1771760	6.36337*
Error	3341173	12	278431.1	
Total	4170570	17	245327.6	
	$F_{1,12,0.10}$=3.17655	**$F_{2,12,0.10}$=2.8068**	**$F_{5,12,0.10}$=2.39402**	

* indicates a significant effect

Table 26: ANOVA analysis of K content of MKF with NaOH treatment.

Source	SS	df	MS	F_{obs}
[NaOH]	32425.07	2	16212.53	23.27455*
Temperature	5465.366	1	5465.366	7.84603*
Interaction	8875.172	2	4437.586	6.37056*
Error	8358.931	12	696.5776	
Total	46765.6	17	2750.918	
	$F_{1,12,0.10}$=3.17655	**$F_{2,12,0.10}$=2.8068**	**$F_{5,12,0.10}$=2.39402**	

* indicates a significant effect.

Table 27: ANOVA analysis of Al content of MKF with NaOH treatment.

Source	SS	df	MS	F_{obs}
[NaOH]	61700.1	2	30850.05	8.77723*
Temperature	15546.44	1	15546.44	4.42316*
Interaction	56074.28	2	28037.14	7.97692*
Error	42177.41	12	3514.784	
Total	133320.8	17	7842.402	
	$F_{1,12,0.10}$=3.17655	**$F_{2,12,0.10}$=2.8068**	**$F_{5,12,0.10}$=2.39402**	

* indicates a significant effect.

Table 28: ANOVA analysis of B content of MKF with NaOH treatment.

Source	SS	df	MS	F_{obs}
[NaOH]	561066.4	2	280533.2	19.23349*
Temperature	4773.049	1	4773.049	0.32724
Interaction	314966.8	2	157483.4	10.79714*
Error	175028	12	14585.66	
Total	880806.2	17	51812.13	
	$F_{1,12,0.10}$=3.17655	**$F_{2,12,0.10}$=2.8068**	**$F_{5,12,0.10}$=2.39402**	

* indicates a significant effect.

Table 29: Summary of ANOVA for major elements of MKF with NaOH treatment.

Element	[NaOH]	Temperature	Interaction
Fe	Effect	No effect	Effect
Ca	Effect	Effect	Effect
Na	Effect	No effect	Effect
Mg	No effect	No effect	Effect
K	Effect	Effect	Effect
Al	Effect	Effect	Effect
B	Effect	No effect	Effect

With the exception of Na, F values were close to the theoretical F value. NaOH concentration had an effect on Fe, Ca, Na, K, Al and B. The temperature did not show an effect on the Fe, Ca, Mg, and B content but showed an effect on Na, K, and Al. The interaction between the NaOH concentration and temperature had a significant effect on the content of all major elements (Fe, Ca, Na, Mg, K, Al, and B).

The temperature had no significant effect on the content of the major elements but when combined with NaOH has an effect. The treatment at the higher temperature reduced the loss in Fe, Ca, Mg, K, and Al when combined with NaOH. It had the opposite effect for Na. There was also an effect from the NaOH concentration. An increase in NaOH concentration decreased the elemental content for Fe, Ca, Na, K, Al, and B. NaOH removal of inorganic content occured but

may be impeded by treatment penetration into the fiber or limited elemental solubility into NaOH solution.

The NaOH treatment had the largest effect on Na. The NaOH concentration, temperature, and their interaction had an effect on Na content. The Na content is high and reflects the NaOH treatment at both temperatures (room temperature and 80°C). This is likely due to O-Na groups being formed on the surface of cellulose. There seems to be a trend of sodium being lower in kenaf treated at an elevated temperature which is reflected by the F_{obs} value for temperature effects.

Table 30 compares elemental content of MKF obtained in this study for the water treatment at room temperature (0-RT) to those reported in the literature for untreated kenaf fibers grown in Malaysia [19]. In comparison to the literature, the elemental content obtained in this thesis differs and is believed to be reflect the differences in growing regions. In particular, potassium is approximately ten times greater in untreated Malaysian kenaf when compared to the kenaf investigated in this study. Mg is also greater in Malaysian kenaf. Na, Ca, Al, and Mn is greater for kenaf in this study. The Ca is over two times greater in this study than in Malaysian kenaf. Fe was not reported for the Malaysian kenaf. It should be noted that silicon was not reported in literature.

Table 30: Comparison of elemental composition of kenaf fibers.

Elements (ppm*)	Literature [19]		This Study
	bast	core	0% at RT
Na	245	81	324
K	2931	2198	280
Ca	1292	1939	4752
Cl	1533	1392	-
Al	325	69	862
Mn	28	9	52
Mg	2801	1271	990
Fe	-	-	505

*Units from this study was converted to ppm (μg/g=ppm).

5.6 Mechanical Properties

The mechanical properties (tensile strength, Young's Modulus, and elongation at break) of MKF-PP composites were assessed in three sets. The first set of composites was prepared to determine the maximum MKF that could be used in the composite for the extrusion system available (Table 31). During extrusion 40MKF-60PP would not flow through the extruder indicating that the maximum MKF concentration to be used with this extruder was 30 wt.% MKF. 30MKF-70PP showed increased tensile strength and Young's Modulus, and decreased elongation at break.

Table 31: Mechanical properties for untreated MKF composites produced during preliminary extrusion experiments to assess maximum MKF content (set 1). Avg ± SD, n=3.

Code	Tensile Strength (MPa)	Elongation at Break (%)	Young's Modulus (MPa)
PP	31.1±0.1	14.4±1.6	495.4±8.9
20MKF-80PP	30.1±1.5	10.0±4.0	586.5±83.1
30MKF-70PP	31.5±2.2	8.7±3.6	646.2±105.6
40MKF-60PP	-	-	-

Set 2 was used to determine the feasibility and the effects of MAPP on the mechanical properties of the MKF-PP composites (Table 33). When compared to composites without MAPP, tensile strength was improved. Young's Modulus increased in composites with 20% MKF but decreased for composites with 30% MKF. The elongation at break was decreased for both 20MKF-77PP-3M, and 30MKF-67PP-3M when compared to composites without MAPP.

Table 32: Mechanical properties for 20MKF-77P-3M and 30MKF-67PP-3M composites produced during preliminary extrusion experiments to assess maximum MKF (set 2). Avg ± SD, n=3.

Code	Tensile Strength (MPa)	Elongation at Break (%)	Young's Modulus (MPa)
20MKF-77PP-3M*	32.0±2.2	8.7±3.2	634.0±96.7
30MKF-67PP-3M*	32.7±2.4	8.5±2.9	635.7±88.7

*M is MAPP

It was determined that 30% MKF should be used and that MAPP should be included in set 3 for assessing the effect of the NaOH treatment. Figure 27 shows the stress-strain curve and the corresponding mechanical properties are summarized in Table 33. The mechanical properties were analyzed by ANOVA and are summarized in Table 34, Table 36 and Table 35.

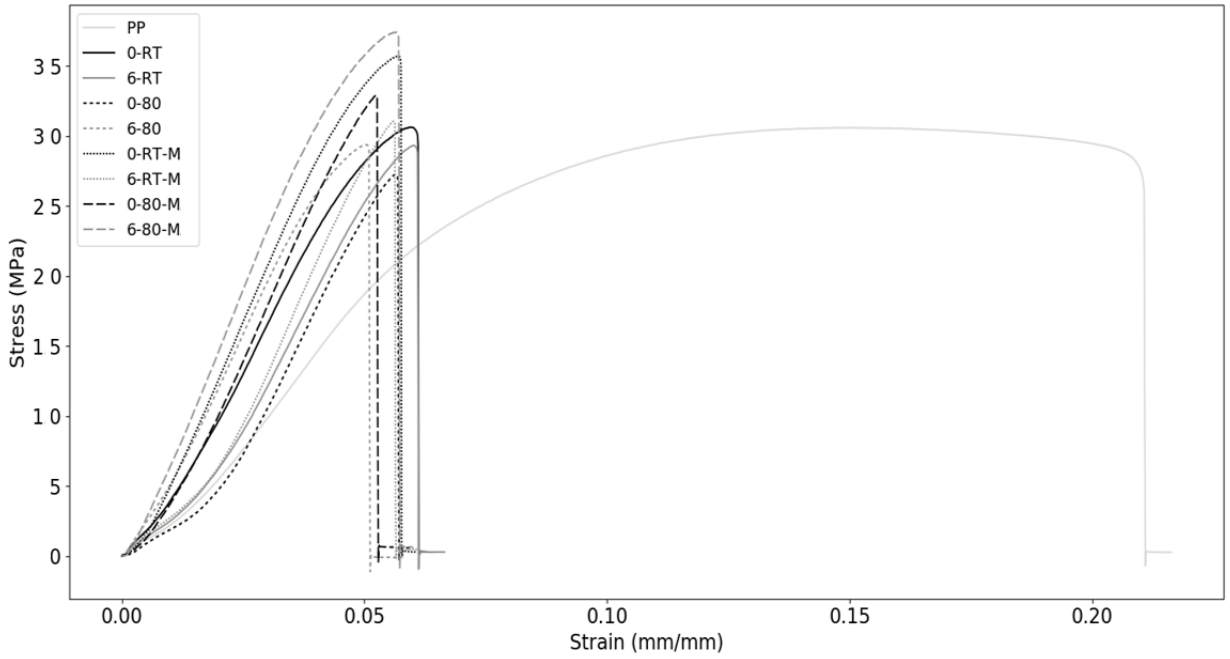

Figure 27: Stress-strain curve of MKF-polypropylene composites treatments and polypropylene grafted maleic anhydride with different NaOH treatments. Avg n=7.

Table 33: Mechanical properties of MKF-PP composites with and without MAPP (M) according to NaOH treatment conditions (set 3). Avg ± SD, n=7.

Code	Tensile Strength at Break (MPa)	Elongation at Break (%)	Young's Modulus (MPa)
PP	30.3 ± 1.3	13.5 ± 2.4	464.2 ± 13.7
0-RT	30.3 ± 0.6	5.8 ± 0.5	665.6 ± 19.7
6-RT	31.3 ± 2.6	6.0 ± 0.4	695.5 ± 49.4
0-RT-M	35.0 ± 1.6	5.8 ± 0.5	770.7 ± 26.0
6-RT-M	31.6 ± 3.7	5.3 ± 0.6	742.1 ± 154.9
0-80	30.5 ± 1.9	5.7 ± 0.6	684.7 ± 73.9
6-80	28.9 ± 2.8	5.1 ± 0.6	710.9 ± 28.7
0-80-M	33.7 ± 1.8	5.6 ± 0.6	764.2 ± 38.0
6-80-M	33.3 ± 3.1	5.4 ± 0.8	765.3 ± 33.5

Table 34: ANOVA analysis of tensile strength for MKF polypropylene composites (set 3).

Source*	Effect	SS	df	MS	F_{obs}
Main Effects					
M	88.424	139.6215	6	23.27025	2.342236*
T	-42.49	32.23929	6	5.373215	0.540834
N	-1.372	0.033614	6	0.005602	0.000564
Interactions					
MxT	-0.372	1.937376	6	0.322896	0.032501
MxN	0.2105	0.620343	6	0.103391	0.010407
TxN	0.089	0.0445	6	0.007417	0.000747
MxTxN	1.4135	27.97175	6	4.661959	0.469243
Error		129.1557	13	9.935057	
				$F_{6,13,0.1}$=2.28	

* M is MAPP, T is temperature, and N is NaOH treatment. * indicates a significant effect.

Using ANOVA with a 90% confidence interval, the addition of MAPP has significant effect on the tensile strength performance of the composite as $F_{obs} > F_{6,13,0.1}$. In contrast, the temperature and concentration of NaOH had no effect on the tensile strength. There was also no effect from the interactions between MAPP concentration, NaOH concentration, and treatment temperature. The presence of MKF and the NaOH treatment did not alter the mechanical properties. The addition of MAPP improved the tensile strength.

Table 35: ANOVA analysis of elongation at break for MKF polypropylene composites (set3).

Source *	Effect	SS	df	MS	F_{obs}
Main Effects					
M	-3.339	0.199088	6	0.033181	0.031924
T	-12.355	2.725822	6	0.454304	0.437083
N	-2.835	0.143522	6	0.02392	0.023014
Interactions					
MxT	0.07625	0.081397	6	0.013566	0.013052
MxN	0.08925	0.111518	6	0.018586	0.017882
TxN	-0.13175	-0.06587	6	-0.01098	-0.01056
MxTxN	0.27075	1.026278	6	0.171046	0.164563
Error		13.5122	13	1.0394	
				$F_{6,13,0.1}$=2.28	

* M is MAPP, T is temperature, and N is NaOH treatment.

Table 36: ANOVA analysis of Young's Modulus for MKF polypropylene composites (set 3).

Source *	Effect	SS	df	MS	F_{obs}
Main Effects					
M	1.99941	0.071386	6	0.011898	0.912884
T	0.04907	4.3E-05	6	7.17E-06	0.00055
N	0.50939	0.004634	6	0.000772	0.059253
Interactions					
MxT	-0.01547	0.003352	6	0.000559	0.04286
MxN	-0.00986	0.001362	6	0.000227	0.017414
TxN	0.006482	0.003241	6	0.00054	0.041449
MxTxN	0.008347	0.000976	6	0.000163	0.012475
Error		0.169431	13	0.013033	
				$F_{6,13,0.1}$=2.28	

* M is MAPP, T is temperature, and N is NaOH treatment.

Table 35 and Table 36 show ANOVA for the elongation at break and the Young's Modulus. NaOH treatments and the addition of MAPP had no effect on these two properties. This shows that the ductility of the material was not affected.

The NaOH treatment of MKF had no effect on the tensile strength, elongation at break and Young's modulus contrary to previous studies. Meon et al. showed that in a composite with kenaf fibers, polypropylene and MAPP in a ratio of 30:67:3, 6% NaOH treatments (performed

for 24 hours at room temperature) improved the tensile strength and the elastic modulus [67]. A somewhat related material from its dimensional properties but of distinct chemical composition, wood flour has also shown improvement with 8% NaOH (treatment time and temperature not stated) treated fiber in a composite (47% wood flour, 47% PP, 3% MAPP, 3% zinc stearate) [68]. The surface protrusions on the MKF surface observed by optical microscopy (5.2) did not alter the tensile strength, elongation at break and Young's modulus of the composite.

5.7 Scanning Electron Microscopy

SEM was used to observe the morphology of the MKF and of the MKF-PP composites. It was also used to observe the interaction between MKF and the polypropylene matrix. These results will be presented and discussed in this section.

Figure 28 shows the effect of NaOH treatments on MKF morphology. Smoothening of MKF surface morphology indicates the removal of impurities such as hemicellulose, lignin, pectin, waxes and oils. The SEM images of MKF fibers show some variation between treatments. The surface of MKF with 0-RT (Figure 28a) shows impurities (indicated by arrows) which may be hemicellulose, lignin, pectin or waxes. At 80°C (Figure 28b), there are still non-cellulosic material present but far less than for room temperature conditions. The decrease of non-cellulosic material at elevated temperatures is similar for fibers treated with 3% NaOH (Figure 28c and d). Non-cellulosic material is present as indicated by the arrow in Figure 28c but there are no noticeable surface non-cellulosic material present in Figure 28d. There is no noticeable difference for non-cellulosic material at 6% between heated (Figure 28f) and unheated

samples (Figure 28e). This mirrors earlier results from optical microscopy (section 5.2) which showed no difference according to temperature for the 6% NaOH treatment.

When comparing MKF at room temperature, there is a gradual removal of surface impurities as indicated by a bumpy surface. At 0% NaOH there is a large amount of surface impurities present. This is reduced when treated with 3% NaOH and almost non-existent with 6% NaOH treatments. With 6% NaOH there is some fibrillation which starts to occur (indicated by arrows in Figure 28e).

When comparing NaOH treatment concentration of MKF at 80°C, there is also a removal of surface impurities with increasing NaOH concentration as indicated by the smoothening of MKF surface. At 0% NaOH there are more impurities than at either 3% or 6% NaOH. 3% NaOH treated MKF has more visible surface impurities than 6% NaOH treated MKF. 6% NaOH treated MKF has no noticeable surface impurities but also has fibrils formed along the surface shown by an arrow in f).

Overall, Figure 28 shows there was a decrease in surface impurities with increasing temperatures at 0% and 3% NaOH. There was also a decrease in surface impurities with increasing NaOH concentration from 0% to 3% NaOH and 3% to 6% NaOH.

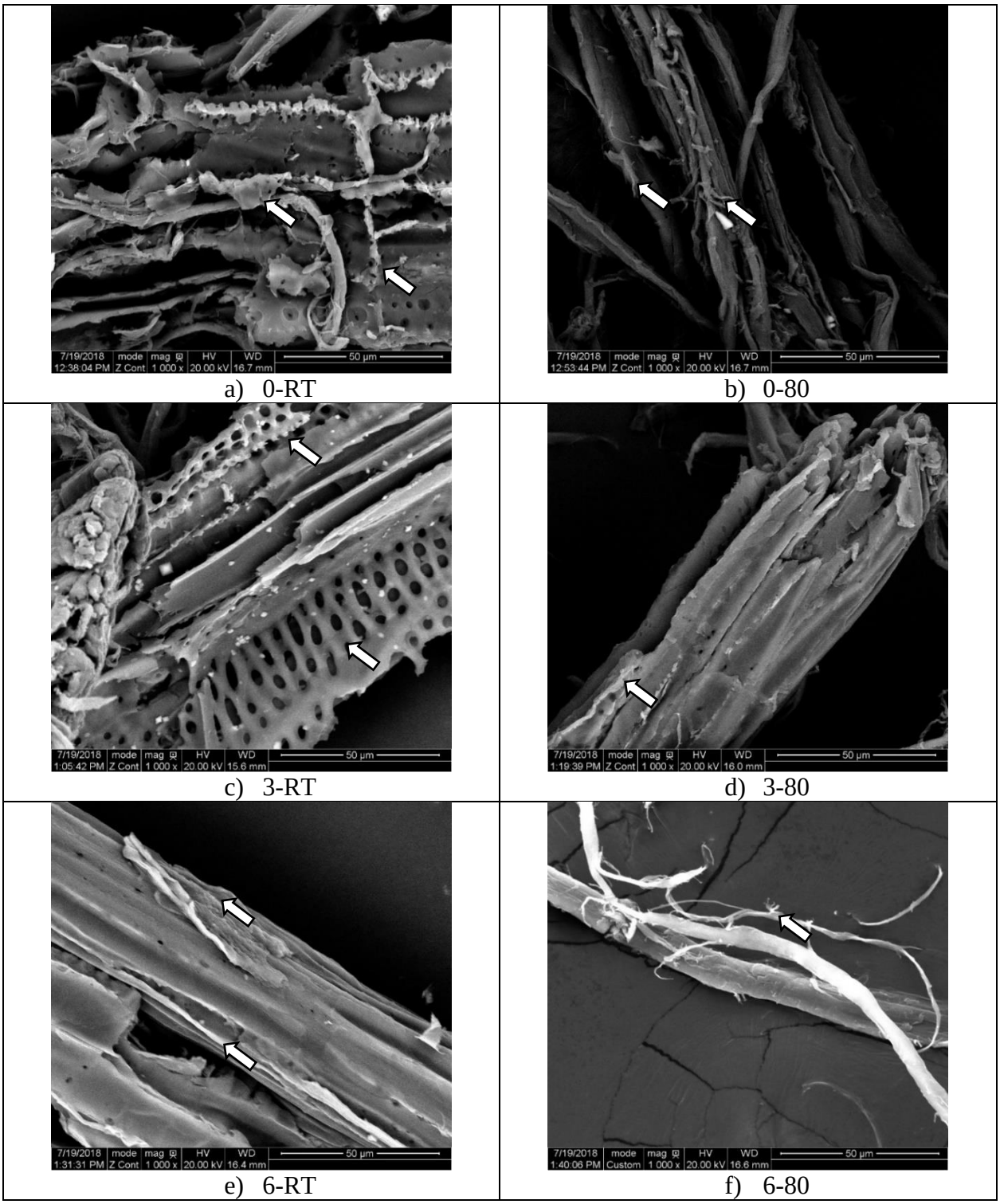

Figure 28: SEM of MKF with varying NaOH treatments a)0% NaOH at room temperature, b) 0% NaOH at 80°C, c) 3% NaOH at room temperature, d) 3% NaOH at 80°C, e)6% NaOH at room temperature, f) 6% NaOH at 80°C.

The effect of the addition of MAPP is pronounced in SEM observations as shown in Figure 29 as fibers can be seen to be coated in the polypropylene matrix (as shown by white arrows) which improves the interfacial adhesion between filler and matrix. In MKF-PP composites without MAPP there are voids between the MKF and the polypropylene matrix (as shown by black arrows). This indicates that MAPP acted as a coupling agent between MKF and polypropylene. MAPP is known to create bonds with hydroxyl groups on the fiber surface and therefore coats the fiber with a hydrophobic polymer layer which aids with fiber wetting and filler-matrix compatibility [54]. This was reflected with the improved mechanical properties (tensile strength, elongation at break and Young's modulus) reported previously in section 5.4. In MKF-PP composites without MAPP, the fracture seemed to have happened because of failure between MKF and PP with the presence of holes where fibers once were. In contrast, for MKF-PP composites containing MAPP, the fracture seemed to have occurred in the PP matrix near the fiber.

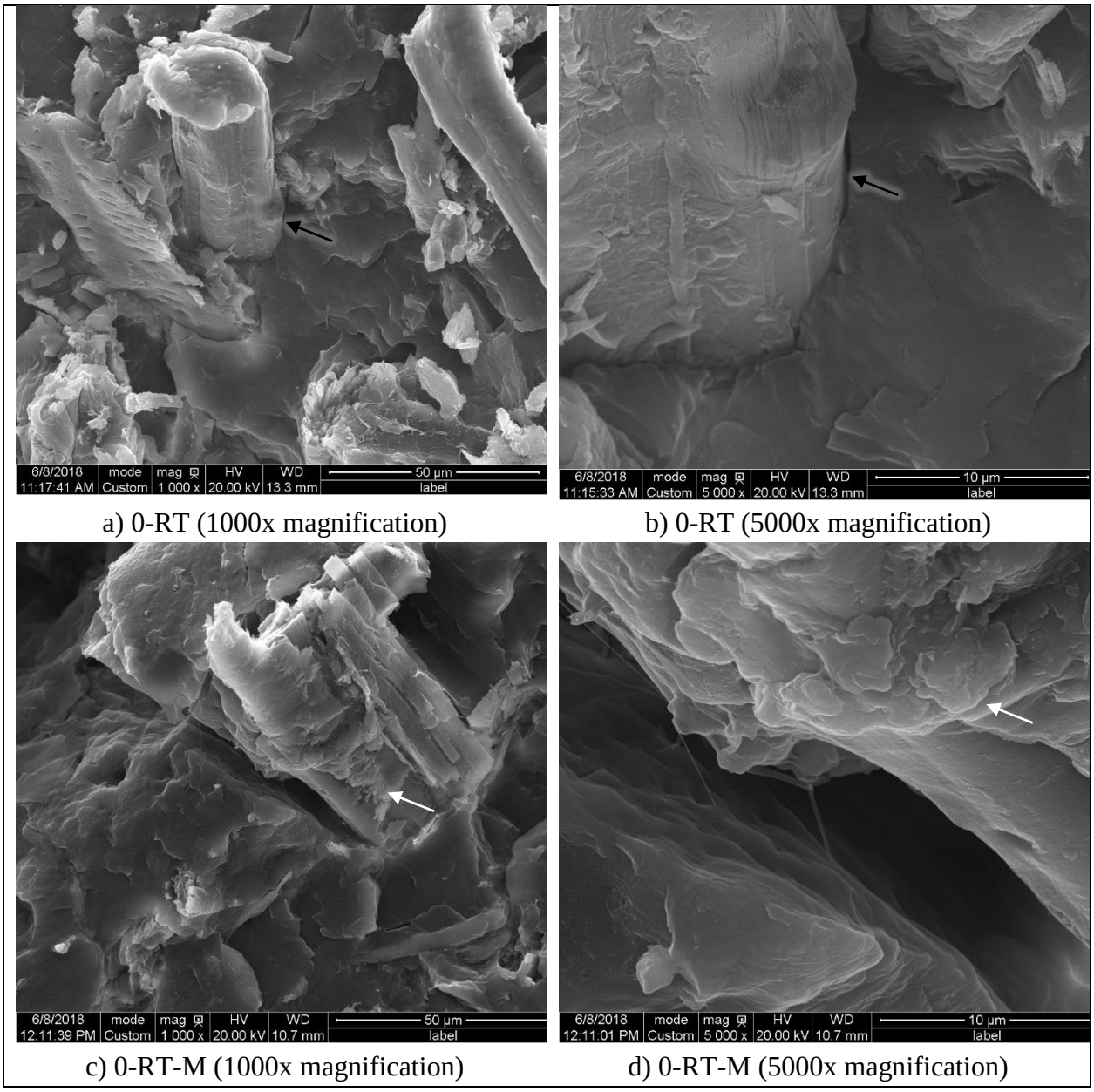

a) 0-RT (1000x magnification) b) 0-RT (5000x magnification)

c) 0-RT-M (1000x magnification) d) 0-RT-M (5000x magnification)

Figure 29: SEM of MKF-PP composites with and without MAPP for MKF in water at room temperature. MKF treated with water at room temperature a) composite without MAPP under 1000x magnification b) composite without MAPP under 5000x magnification, c) composite with MAPP under 1000x magnification, d) composite with MAPP under 5000x magnification.

The effect of the NaOH treatments on MKF observed by SEM for MKF-PP composites is less pronounced as shown in Figure 30 as it is difficult to differentiate between NaOH treatments. When comparing composites with MKF treated at room temperature and 80°C, there was no noticeable differences between the NaOH treatments. When comparing composites with MKF treated at room temperature, 0% NaOH treatment (Figure 30 a) and 6% NaOH treatment (Figure 30c) no noticeable difference could be detected. When comparing composites with MKF treated at 80°C, 0% NaOH (Figure 30 b) and 6% NaOH treated samples (Figure 30 d) also showed no noticeable difference between each other. All MKF-PP composites showed voids between fiber and polypropylene as shown by arrows in Figure 30 a)-d).

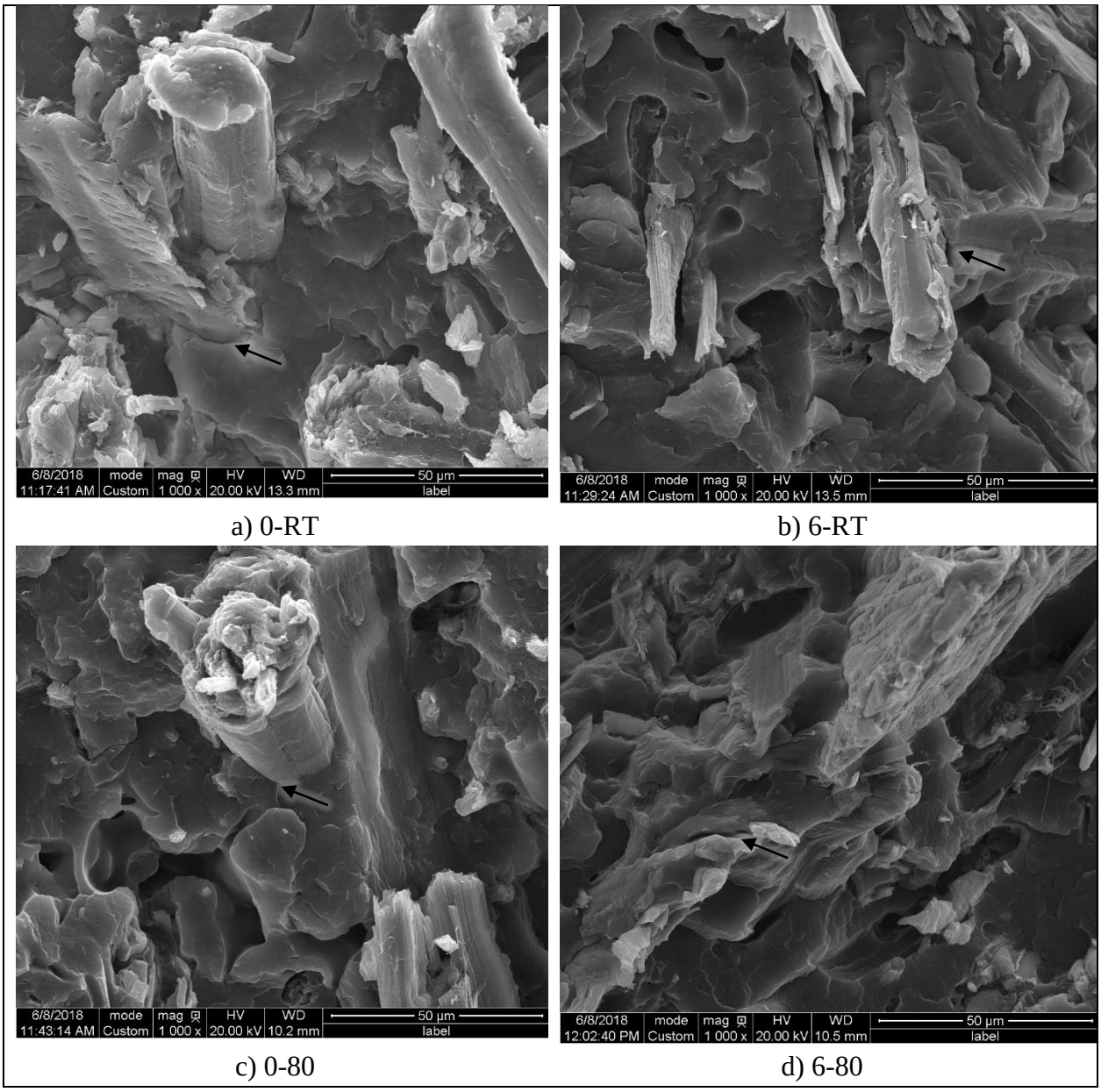

Figure 30: SEM images of MKF-PP without MAPP for different NaOH treatments of MKF at room temperature (RT) and 80°C. a) 0% NaOH at room temperature, b) 6% NaOH at room temperature, c) 0% NaOH at 80°C, d) 6% NaOH at 80°C.

The expected effect of the NaOH treatments was to obtain a roughened surface with increasing treatment conditions as well as enhanced fiber wetting with the matrix and fewer voids. However, the process of milling the fiber with a centrifugal mill may also have induced roughening of the fibers to appear roughened as shown in Figure 30 a) so it is not possible to make conclusions on the effect of NaOH treatment and the roughening of MKF fibers.

5.8 Energy Dispersive X-Ray Spectroscopy

SEM scans of MKF and MKF-PP (with and without MAPP) composite fracture were further analyzed by energy dispersive X-ray spectroscopy (EDX) to obtain mapping of elements. The elemental analysis of the surface of the selected area of a sample could be scanned to a depth of up to 1-2 μm. Note that the limit of detection for EDX (~1000 ppm) is higher than ICP and provides surface mapping [93]. The EDX analysis are shown in Table 37 for MKF, and Table 38 and Figure 31 for MKF-PP composites. Detectable elements were carbon, oxygen, silicon, and calcium.

The EDX analysis of MKF with NaOH treatments (Table 37) showed only carbon and oxygen. There was no silicon and calcium detected on the surface of the fibers which indicates that inorganic content was removed from the surface of MKF.

Table 37: EDX analysis of MKF with various NaOH treatments.

	Weight %					
Element	**0-RT**	**0-80**	**3-RT**	**3-80**	**6-RT**	**6-80**
C	58.6	53.2	58.2	62.3	63.8	71.4
O	41.4	46.8	41.8	37.7	36.2	28.6

Table 38 shows the EDX analysis of MKF-PP composite (with and without MAPP) cross-sections. Figure 31 shows the mapping of elements of the cross-sectional area of the 0-RT composite. Mapping was performed on 0-RT composite as it contained silicon and calcium, but mapping was not performed on other composites.

Table 38: EDX analysis of the cross-section of MKF-PP composites and the effect of NaOH treatment.

	Weight%							
Element	**0-RT**	**6-RT**	**0-80**	**6-80**	**0-RT-M**	**6-RT-M**	**0-80-M**	**6-80-M**
C	62.7	72.4	81.4	80.2	76.3	72.9	72.1	81.9
O	31.3	27.6	18.6	19.8	23.8	27.1	27.9	18.1
Si	2.7	-	-	-	-	-	-	-
Ca	3.3	-	-	-	-	-	-	-

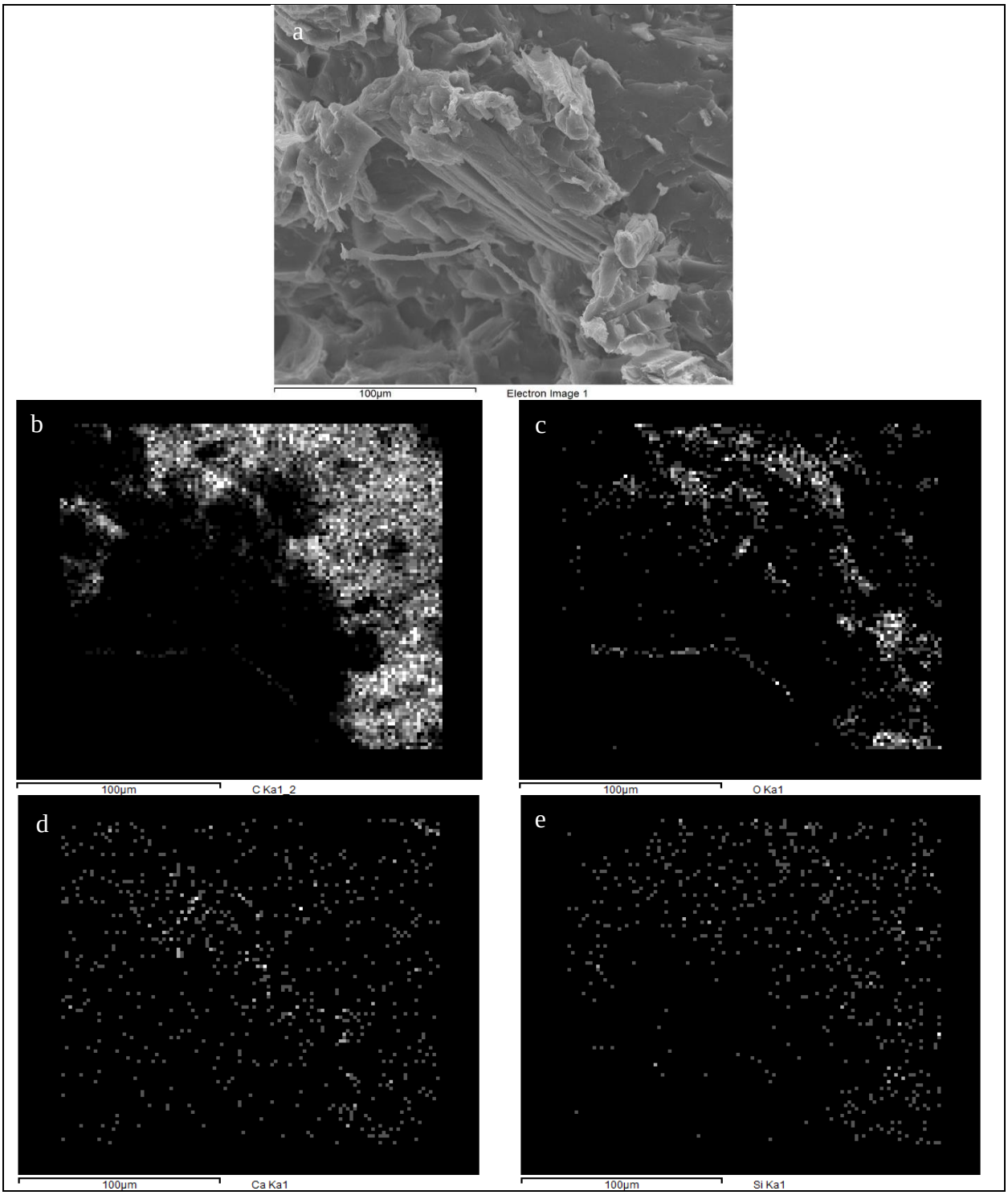

Figure 31: EDX mapping of MKF-PP composite (0-RT) without MAPP. a) SEM image, b) carbon, c) oxygen, d) calcium, e) silicon.

The major elements detected in the MKF-PP (with and without MAPP) composites were carbon and oxygen. Carbon is present in all composite constituents (MKF, polypropylene and MAPP). Oxygen indicates the presence of MKF and MAPP as polypropylene lacks the presence of the element. When comparing treatment temperature in composites without MAPP, 0-RT MKF-PP composite, had higher oxygen levels when compared to 0-80 MKF-PP composite. This indicates that there was less fiber in the selected sample image at 80^{o}C. This is not unusual as the sample image size is very small (less than 300 μm wide). This was also seen in composites treated with 6% NaOH (6-RT and 6-80).

When comparing treatment temperature in composites with MAPP, composites with 0% NaOH treated MKF had lower oxygen levels when MKF was treated at room temperature (0-RT-M) than 80°C (0-80-M). Composites treated with 6% NaOH treated MKF had higher oxygen levels when using MKF treated at room temperature (6-RT-M) compared to those using MKF treated at 80°C (6-80-M). Higher oxygen suggests that there were more fibers or MAPP present on the surface of the sample fracture surface.

Comparison may also be made based on MKF NaOH treatment concentration at a specific temperature. When comparing composites without MAPP, composites with MKF treated at room temperature (0-RT) had higher oxygen level than 6-RT. At 80°C, the MKF-PP composite (0-80) had lower oxygen level than the MKF-PP composite (6-80). In composites with MAPP, the MKF-PP composite with room temperature 0% NaOH treated MKF (0-RT-M) had lower oxygen level than 6-RT-M. The MKF-PP composite with MKF treated at 80°C with 0% NaOH (0-80-M) has higher oxygen levels than composites treated with 6% NaOH (6-80-M).

When comparing the effect of MAPP content in MKF-PP composites, 0-RT, 6-RT, and 6-80 had higher oxygen level compared to those composites containing MAPP (0-RT-M, 6-RT-M, and 6-80-M). This is proposed to be from MAPP coating the surface of fibers with non-oxygen containing polypropylene. The MKF-PP composite 0-80, on the other hand, has lower oxygen levels when compared to 0-80-M. The difference in carbon and oxygen content estimated from EDX reflects the lack of homogeneity of the composite mixture and the limitation of the analysis.

Silicon, and calcium content of the composites was detected only for the 0-RT treatment conditions. 0-RT does not contain MAPP. This shows that treatments at 80^{o}C and treatments with NaOH removed the silicon and calcium present at the surface of the fiber. The MKF-PP composite, 0-RT, as shown in Figure 31 has 3.33% calcium and 2.67% silicon. Figure 31a) shows the regions in which carbon is found in MKF-PP (0-RT) composite. There are dark regions where carbon was not detected which may reflect the topography of the surface. The surface is not flat and as a result an electron shadow is formed preventing areas from being scanned sufficiently. Oxygen should only be present in the kenaf filler since polypropylene does not contain oxygen. The map of oxygen shows detectable areas of kenaf.

When comparing MKF-PP composites with and without MAPP, there is a decrease in the silicon and calcium content present when treated with 0% NaOH at room temperature. This implies that the MAPP may coat the fiber and interfere with the detection of silicon and calcium at the surface. It should be noted that EDX analysis is for a small area of the composite, which was assumed to be a representative area but may not always be realistic.

Combining EDX analysis with the mechanical properties presented previously (tensile strength, Young's modulus, and elongation at break) show no evidence that the silicon and calcium content affected composite performance. If the silicon and calcium content were to alter mechanical performance, we would expect a difference in the mechanical properties for 0-RT and 0-RT-M when compared to other composites.

5.9 Conclusions

Kenaf was milled to have lengths that were predominantly below 1.5 mm. The effect of sodium hydroxide treatments on the inorganic content of kenaf was assessed by optical microscopy, thermogravimetric analysis, and inductively-coupled plasma optical emission spectroscopy. The NaOH concentration and temperature (0% NaOH at 80°C, 3% NaOH at room temperature and 80°C, and 6% NaOH at room temperature and 80°C) increased thin protrusions on the surface of milled kenaf fibers (MKF). This implies that the cellulose microfibrils became visible suggesting that the hemicellulose constituents surrounding the microfibrils were removed. SEM showed surface smoothening of cellulose in samples with increasing NaOH concentration (3% and 6%) and temperature (80°C), suggesting cellulose extraction. This is supported by TGA analysis which showed the disappearance of the hemicellulose shoulder (at 240-325°C) of the DTG curve of all 3% and 6% NaOH treated kenaf. Chemical composition analysis also confirmed that there was removal of 12-37% hemicellulose with NaOH treatment.

The inorganic content, obtained by ICP, showed the presence of inorganic content in MKF. Six elements, iron, calcium, sodium, magnesium, boron and potassium were present in quantities

above 150 μg/g and classified as major elements. Fourteen other elements were present at concentrations below 150 μg/g and were classified as minor elements. These major and minor elements made up 0.76-0.94 wt% of MKF. Of the major elements, NaOH concentrations affected Fe, Ca, Na, K, Al and B content. Treatment temperature affected Na, K and Al content. The interaction between NaOH concentration and treatment temperature affected all major elements.

The sodium content increased with increasing sodium hydroxide concentration which suggest that the washing step may not have been efficient. ICP data also indicated that over 80% of inorganic content was retained after NaOH treatment. EDX analysis of the MKF showed the presence of carbon and oxygen with no detectable levels of inorganic content. This indicates that there was little, if any, inorganic content located on the surface of MKF.

Composites were made with MKF and polypropylene, with and without MAPP. The tensile strength (28.9-30.3 MPa), elongation at break (5.1-6.0%), and Young's modulus (665.5-710.9 MPa) of composites (with and without MAPP) showed that the sodium hydroxide treatment of MKF did not affect these properties. SEM of the fractured composites showed poor MKF wetting and interfacial interaction by the polymer. Silicon was detected on the MKF surface for composites made of 30% room temperature water treated MKF and 70% polypropylene.

MAPP was also incorporated in the composite. The addition MAPP improved tensile strength (31.6-35.0 MPa) but did not improve elongation at break or Young's modulus. MAPP improved the tensile strength by coating the MKF as shown in SEM imaging. MAPP caused fractures to occur in the matrix instead of the MKF-PP interface. Therefore, the addition of

MAPP is recommended. There was no evidence to indicate that the mechanical properties, NaOH treatment, or the addition of MAPP of kenaf-PP composites changed with surface inorganic content.

Based on the work presented in this thesis examining the inorganic content on the mechanical properties of MKF-PP composites, future work should address the following:

- The effect of NaOH treatments at current and higher concentrations and temperature on cellulose, hemicellulose, lignin, and inorganic content.
- The effect of NaOH treatments at current and higher concentrations and temperature on mechanical performance.
- The use of the native inorganic content for inorganic impregnation in kenaf-polypropylene composite.
    - The inorganic content may be used as a nucleation site for the polymer matrix.

References

[1] Office of the Press Secretary, "President Obama Announces Historic 54.5 mpg Fuel Efficiency Standard," *The White House President Barack Obama*, 29-Jul-2011. [Online]. Available: https://obamawhitehouse.archives.gov/the-press-office/2011/07/29/president-obama-announces-historic-545-mpg-fuel-efficiency-standard. [Accessed: 13-Jun-2017].

[2] United States Department of Transportation, "Table 4- 23. Average Fuel Efficiency of U.S. Light Duty Vehicles," *Bureau of Transportation Statistics*. [Online]. Available: https://www.rita.dot.gov/bts/sites/rita.dot.gov.bts/files/publications/national_transportation_statistics/html/table_04_23.html. [Accessed: 13-Jun-2017].

[3] Economics & Statistics Division, "Plastics and Polymer Composites in Light Vehicle," American Chemistry Council, 2016.

[4] G. Marsh, "Next step for automotive materials," *Mater. Today*, vol. 6, no. 4, pp. 36–43, Apr. 2003.

[5] "Natural Fiber Composites Market Size | NFC Industry Report, 2018-2024." [Online]. Available: https://www.grandviewresearch.com/industry-analysis/natural-fiber-composites-market. [Accessed: 01-Jun-2018].

[6] R. D. S. G. Campilho, *Natural Fiber Composites*. CRC Press, 2015.

[7] X. Li, L. G. Tabil, and S. Panigrahi, "Chemical Treatments of Natural Fiber for Use in Natural Fiber-Reinforced Composites: A Review," *J. Polym. Environ.*, vol. 15, no. 1, pp. 25–33, Feb. 2007.

[8] J. Holbery and D. Houston, "Natural-fiber-reinforced polymer composites in automotive applications," *JOM*, vol. 58, no. 11, pp. 80–86, Nov. 2006.

[9] D. B. Dittenber and H. V. S. GangaRao, "Critical review of recent publications on use of natural composites in infrastructure," *Compos. Part Appl. Sci. Manuf.*, vol. 43, no. 8, pp. 1419–1429, Aug. 2012.

[10] L. Mohammed, M. N. M. Ansari, G. Pua, M. Jawaid, and M. S. Islam, "A Review on Natural Fiber Reinforced Polymer Composite and Its Applications," *International Journal of Polymer Science*, 2015. [Online]. Available: https://www.hindawi.com/journals/ijps/2015/243947/. [Accessed: 01-Jun-2018].

[11] M. Saxena, A. Pappu, A. Sharma, R. Haque, and S. Wankhede, *Composite Materials from Natural Resources: Recent Trends and Future Potentials*. 2011.

[12] Flax Council of Canada, "Chapter 12: Flax Straw and Fibre," in *Growing Flax-Production, Management & Diagnostic Guide*, 2015.

[13] Statistics Canada, "Field and special crops (Seeded area)," 04-Oct-2017. [Online]. Available: http://www.statcan.gc.ca/tables-tableaux/sum-som/l01/cst01/prim11a-eng.htm. [Accessed: 10-Apr-2018].

[14] Alberta Agriculture and Forestry, "Industrial Hemp Enterprise," *Alberta Agriculture and Forestry*. [Online]. Available: https://www1.agric.gov.ab.ca/$department/deptdocs.nsf/all/agdex126. [Accessed: 10-Apr-2018].

[15] N. Bertoniere *et al.*, *Cotton Fiber Chemistry and Technology*, 1st ed. 15 December 2006: CRC Press.
[16] C. Goussé, H. Chanzy, M. L. Cerrada, and E. Fleury, "Surface silylation of cellulose microfibrils: preparation and rheological properties," *Polymer*, vol. 45, no. 5, pp. 1569–1575, Mar. 2004.
[17] M. Z. Rong, M. Q. Zhang, Y. Liu, G. C. Yang, and H. M. Zeng, "The effect of fiber treatment on the mechanical properties of unidirectional sisal-reinforced epoxy composites," *Compos. Sci. Technol.*, vol. 61, no. 10, pp. 1437–1447, Aug. 2001.
[18] H. Deka, M. Misra, and A. Mohanty, "Renewable resource based 'all green composites' from kenaf biofiber and poly(furfuryl alcohol) bioresin," *Ind. Crops Prod.*, vol. 41, pp. 94–101, Jan. 2013.
[19] A. Ashori, J. Harun, W. D. Raverty, and M. N. M. Yusoff, "Chemical and Morphological Characteristics of Malaysian Cultivated Kenaf (Hibiscus cannabinus) Fiber," *Polym.-Plast. Technol. Eng.*, vol. 45, no. 1, pp. 131–134, Feb. 2006.
[20] A. Hao, H. Zhao, and J. Y. Chen, "Kenaf/polypropylene nonwoven composites: The influence of manufacturing conditions on mechanical, thermal, and acoustical performance," *Compos. Part B Eng.*, vol. 54, pp. 44–51, Nov. 2013.
[21] N. Reddy and Y. Yang, "Properties and potential applications of natural cellulose fibers from the bark of cotton stalks," *Bioresour. Technol.*, vol. 100, no. 14, pp. 3563–3569, Jul. 2009.
[22] L. Y. Mwaikambo and M. P. Ansell, "Chemical modification of hemp, sisal, jute, and kapok fibers by alkalization," *J. Appl. Polym. Sci.*, vol. 84, no. 12, pp. 2222–2234, Jun. 2002.
[23] N. Reddy and Y. Yang, "Extraction and characterization of natural cellulose fibers from common milkweed stems," *Polym. Eng. Sci.*, vol. 49, no. 11, pp. 2212–2217, Nov. 2009.
[24] P. Gu, R. K. Hessley, and W.-P. Pan, "Thermal characterization analysis of milkweed flos," *J. Anal. Appl. Pyrolysis*, vol. 24, no. 2, pp. 147–161, Dec. 1992.
[25] N. G. Jústiz-Smith, G. J. Virgo, and V. E. Buchanan, "Potential of Jamaican banana, coconut coir and bagasse fibres as composite materials," *Mater. Charact.*, vol. 59, no. 9, pp. 1273–1278, Sep. 2008.
[26] T. Qu, W. Guo, L. Shen, J. Xiao, and K. Zhao, "Experimental Study of Biomass Pyrolysis Based on Three Major Components: Hemicellulose, Cellulose, and Lignin," *Ind. Eng. Chem. Res.*, vol. 50, no. 18, pp. 10424–10433, Sep. 2011.
[27] H. Chen, *Biotechnology of Lignocellulose - Theory and Practice*, 1st ed. Springer Netherlands, 2014.
[28] B. Alberts, A. Johnson, J. Lewis, M. Raff, K. Roberts, and P. Walter, "The Plant Cell Wall," 2002.
[29] I. Rezić, M. Zeiner, and I. Steffan, "Determination of 28 selected elements in textiles by axially viewed inductively coupled plasma optical emission spectrometry," *Talanta*, vol. 83, no. 3, pp. 865–871, Jan. 2011.
[30] "Standards & Methods." [Online]. Available: https://www.tappi.org/Publications-Standards/Standards-Methods/. [Accessed: 10-Sep-2018].
[31] admin, "Fiber Analyzer A2000," *ANKOM Technology*, 03-Sep-2014. [Online]. Available: https://www.ankom.com/analytical-methods-support/fiber-analyzer-a2000. [Accessed: 10-Sep-2018].

[32] M. Bourguignon, K. J. Moore, R. C. Brown, K. H. Kim, B. S. Baldwin, and R. Hintz, "Variety Trial and Pyrolysis Potential of Kenaf Grown in Midwest United States," *BioEnergy Res.*, vol. 10, no. 1, pp. 36–49, Mar. 2017.
[33] M. Jonoobi, J. Harun, M. Mishra, and K. Oksman, "Chemical composition, crystallinity and thermal degradation of bleached and unbleached kenaf bast (Hibiscus cannabinus) pulp and nanofiber," *BioResources*, vol. 4, no. 2, pp. 626–639, 2009.
[34] S. J. J. Lips, G. M. Iñiguez de Heredia, R. G. M. Op den Kamp, and J. E. G. van Dam, "Water absorption characteristics of kenaf core to use as animal bedding material," *Ind. Crops Prod.*, vol. 29, no. 1, pp. 73–79, Jan. 2009.
[35] N. I. Wan Azelee, J. Md Jahim, A. Rabu, A. M. Abdul Murad, F. D. Abu Bakar, and R. Md Illias, "Efficient removal of lignin with the maintenance of hemicellulose from kenaf by two-stage pretreatment process," *Carbohydr. Polym.*, vol. 99, pp. 447–453, Jan. 2014.
[36] W. Soboyejo, *Mechanical Properties of Engineered Materials*. CRC Press, 2002.
[37] "Elongation at break." [Online]. Available: http://www.ensinger.in/en/general-information/technical-information/properties-of-plastics/mechanical-properties/elongation-at-break/. [Accessed: 24-Jan-2018].
[38] C. I. Idumah and A. Hassan, "Emerging trends in flame retardancy of biofibers, biopolymers, biocomposites, and bionanocomposites," *Rev. Chem. Eng.*, vol. 32, no. 1, pp. 115–148, 2015.
[39] A. Athijayamani, M. Thiruchitrambalam, U. Natarajan, and B. Pazhanivel, "Effect of moisture absorption on the mechanical properties of randomly oriented natural fibers/polyester hybrid composite," *Mater. Sci. Eng. A*, vol. 517, no. 1–2, pp. 344–353, Aug. 2009.
[40] O. Faruk, A. K. Bledzki, H.-P. Fink, and M. Sain, "Biocomposites reinforced with natural fibers: 2000–2010," *Prog. Polym. Sci.*, vol. 37, no. 11, pp. 1552–1596, Nov. 2012.
[41] H. Ku, H. Wang, N. Pattarachaiyakoop, and M. Trada, "A review on the tensile properties of natural fiber reinforced polymer composites," *Compos. Part B Eng.*, vol. 42, no. 4, pp. 856–873, Jun. 2011.
[42] "Izod Impact (Notched) ASTM D256, ISO 180." [Online]. Available: http://www.intertek.com/polymers/testlopedia/notched-izod-impact-astm-d256/. [Accessed: 13-Sep-2018].
[43] ASTM International, "ASTM D256-10e1 Standard Test Methods for Determining the Izod Pendulum Impact Resistance of Plastics." ASTM International, 2015.
[44] I. S. Aji, E. S. Zainudin, K. Abdan, S. M. Sapuan, and M. D. Khairul, "Mechanical properties and water absorption behavior of hybridized kenaf/pineapple leaf fibre-reinforced high-density polyethylene composite," *J. Compos. Mater.*, vol. 47, no. 8, pp. 979–990, Apr. 2013.
[45] I. Ali, K. Jayaraman, and D. Bhattacharyya, "Effects of resin and moisture content on the properties of medium density fibreboards made from kenaf bast fibres," *Ind. Crops Prod.*, vol. 52, pp. 191–198, Jan. 2014.
[46] N. Okuda and M. Sato, "Manufacture and mechanical properties of binderless boards from kenaf core," *J. Wood Sci.*, vol. 50, no. 1, pp. 53–61, Feb. 2004.

[47] I. S. Aji, S. M. Sapuan, E. S. Zainudin, and K. Abdan, “Kenaf Fibres as Reinforcement for Polymeric Composites: a Review,” *Int. J. Mech. Mater. Eng.*, vol. 4, no. 3, pp. 239–248, 2009.
[48] P. J. LeMahieu, E. S. Oplinger, and D. H. Putnam, “Kenaf,” *Alternative Field Crops Manual, Purdue University*, 1991. [Online]. Available: https://hort.purdue.edu/newcrop/afcm/kenaf.html. [Accessed: 06-Apr-2018].
[49] “Goldco International Inc.” [Online]. Available: http://www.goldcointernationalinc.com/. [Accessed: 18-Sep-2017].
[50] M. T. Paridah, A. Abdelrhman, and M. Shahwahid, “Cost Benefit Analysis of Kenaf Cultivation for Producing Fiber in Malaysia,” *Arab. J. Bus. Manag. Rev.*, vol. 7, no. 5, 2017.
[51] M. Barth and M. Carus, “Carbon Footprint and Sustainability of Different Natural Fibres for Biocomposites and Insulation Material.” nova Institue, 2015.
[52] M. Kostic, B. Pejic, and P. Skundric, “Quality of chemically modified hemp fibers,” *Bioresour. Technol.*, vol. 99, no. 1, pp. 94–99, Jan. 2008.
[53] B. D. Lazić *et al.*, “Influence of hemicelluloses and lignin content on structure and sorption properties of flax fibers,” *Cellulose*, vol. 25, no. 1, pp. 697–709, Jan. 2018.
[54] M. M. Kabir, H. Wang, K. T. Lau, and F. Cardona, “Chemical treatments on plant-based natural fibre reinforced polymer composites: An overview,” *Compos. Part B Eng.*, vol. 43, no. 7, pp. 2883–2892, Oct. 2012.
[55] D. O. Krause *et al.*, “Opportunities to improve fiber degradation in the rumen: microbiology, ecology, and genomics,” *FEMS Microbiol. Rev.*, vol. 27, no. 5, pp. 663–693, Dec. 2003.
[56] A. M. M. Edeerozey, H. M. Akil, A. B. Azhar, and M. I. Z. Ariffin, “Chemical modification of kenaf fibers,” *Mater. Lett.*, vol. 61, no. 10, pp. 2023–2025, Apr. 2007.
[57] Y. Xie, C. A. S. Hill, Z. Xiao, H. Militz, and C. Mai, “Silane coupling agents used for natural fiber/polymer composites: A review,” *Compos. Part Appl. Sci. Manuf.*, vol. 41, no. 7, pp. 806–819, Jul. 2010.
[58] American Chemistry Council, “Plastics and Polymer Composites in Light Vehicles,” 2017.
[59] C. Maier and T. Calafut, *Polypropylene: The Definitive User’s Guide and Databook*. William Andrew, 1998.
[60] R. B. Rosner, “Conductive materials for ESD applications: an overview,” in *Electrical Overstress/Electrostatic Discharge Symposium Proceedings*, 2000, pp. 121–131.
[61] S. Advani and K.-T. Hsiao, *Manufacturing Techniques for Polymer Matrix Composites (PMCs)*. Woodhead Publishing, 2012.
[62] K. L. Pickering, M. G. A. Efendy, and T. M. Le, “A review of recent developments in natural fibre composites and their mechanical performance,” *Compos. Part Appl. Sci. Manuf.*, vol. 83, pp. 98–112, Apr. 2016.
[63] R. O. Ritchie, “The conflicts between strength and toughness,” *Nat. Mater.*, vol. 10, no. 11, pp. 817–822, Nov. 2011.
[64] M. Ho *et al.*, “Critical factors on manufacturing processes of natural fibre composites,” *Compos. Part B Eng.*, vol. 43, no. 8, pp. 3549–3562, Dec. 2012.

[65] A. Subasinghe and D. Bhattacharyya, “Performance of different intumescent ammonium polyphosphate flame retardants in PP/kenaf fibre composites,” *Compos. Part Appl. Sci. Manuf.*, vol. 65, pp. 91–99, Oct. 2014.
[66] M. N. Ichazo, C. Albano, J. González, R. Perera, and M. V. Candal, “Polypropylene/wood flour composites: treatments and properties,” *Compos. Struct.*, vol. 54, no. 2, pp. 207–214, Nov. 2001.
[67] M. S. Meon, M. F. Othman, H. Husain, M. F. Remeli, and M. S. M. Syawal, “Improving Tensile Properties of Kenaf Fibers Treated with Sodium Hydroxide,” *Procedia Eng.*, vol. 41, pp. 1587–1592, Jan. 2012.
[68] P.-Y. Kuo, S.-Y. Wang, J.-H. Chen, H.-C. Hsueh, and M.-J. Tsai, “Effects of material compositions on the mechanical properties of wood–plastic composites manufactured by injection molding,” *Mater. Des.*, vol. 30, no. 9, pp. 3489–3496, Oct. 2009.
[69] O. Hosseinaei, S. Wang, A. A. Enayati, and T. G. Rials, “Effects of hemicellulose extraction on properties of wood flour and wood–plastic composites,” *Compos. Part Appl. Sci. Manuf.*, vol. 43, no. 4, pp. 686–694, Apr. 2012.
[70] K. Sever, M. Sarikanat, Y. Seki, G. Erkan, and Ü. H. Erdoğan, “The Mechanical Properties of γ-Methacryloxypropyltrimethoxy silane-treated Jute/Polyester Composites,” *J. Compos. Mater.*, vol. 44, no. 15, pp. 1913–1924, Jul. 2010.
[71] J. Shi, S. Q. Shi, H. M. Barnes, M. F. Horstemeyer, and G. Wang, “Kenaf Bast Fibers—Part II: Inorganic Nanoparticle Impregnation for Polymer Composites,” *Int. J. Polym. Sci.*, vol. 2011, p. e736474, Sep. 2011.
[72] A. W. Coats and J. P. Redfern, “Thermogravimetric analysis. A review,” *Analyst*, vol. 88, no. 1053, pp. 906–924, Jan. 1963.
[73] H. Yang, R. Yan, H. Chen, D. H. Lee, and C. Zheng, “Characteristics of hemicellulose, cellulose and lignin pyrolysis,” *Fuel*, vol. 86, no. 12, pp. 1781–1788, Aug. 2007.
[74] F. Yao, Q. Wu, Y. Lei, W. Guo, and Y. Xu, “Thermal decomposition kinetics of natural fibers: Activation energy with dynamic thermogravimetric analysis,” *Polym. Degrad. Stab.*, vol. 93, no. 1, pp. 90–98, Jan. 2008.
[75] D. Zheng, R.-Y. Ding, Z. Lei, Z. Xingqun, and Y. Chong-Wen, “Thermal properties of flax fiber scoured by different methods,” *Therm. Sci.*, vol. 19, pp. 5–5, Jan. 2014.
[76] A. A. Yussuf, I. Massoumi, and A. Hassan, “Comparison of Polylactic Acid/Kenaf and Polylactic Acid/Rise Husk Composites: The Influence of the Natural Fibers on the Mechanical, Thermal and Biodegradability Properties,” *J. Polym. Environ.*, vol. 18, no. 3, pp. 422–429, Sep. 2010.
[77] A. Arbelaiz, G. Cantero, B. Fernández, I. Mondragon, P. Gañán, and J. M. Kenny, “Flax fiber surface modifications: Effects on fiber physico mechanical and flax/polypropylene interface properties,” *Polym. Compos.*, vol. 26, no. 3, pp. 324–332, Jun. 2005.
[78] M. Hughes, G. Sèbe, J. Hague, C. Hill, M. Spear, and L. Mott, “An investigation into the effects of micro-compressive defects on interphase behaviour in hemp-epoxy composites using half-fringe photoelasticity,” *Compos. Interfaces*, vol. 7, no. 1, pp. 13–29, Jan. 2000.
[79] J. Kuo, “Electron microscopy: methods and protocols - Scholars Portal Books,” 2007. [Online]. Available: http://books1.scholarsportal.info.proxy.lib.uwaterloo.ca/viewdoc.html?id=/ebooks/ebooks2/springer/2011-04-29/1/9781597452946. [Accessed: 09-Feb-2018].

[80] P. J. Herrera-Franco and A. Valadez-González, “A study of the mechanical properties of short natural-fiber reinforced composites,” *Compos. Part B Eng.*, vol. 36, no. 8, pp. 597–608, Dec. 2005.
[81] I. Aranberri-Askargorta, T. Lampke, and A. Bismarck, “Wetting behavior of flax fibers as reinforcement for polypropylene,” *J. Colloid Interface Sci.*, vol. 263, no. 2, pp. 580–589, Jul. 2003.
[82] S.-J. Kim, J.-B. Moon, G.-H. Kim, and C.-S. Ha, “Mechanical properties of polypropylene/natural fiber composites: Comparison of wood fiber and cotton fiber,” *Polym. Test.*, vol. 27, no. 7, pp. 801–806, Oct. 2008.
[83] Ametek Materials Analysis Division, “Energy Dispersive Spectroscopy.” Ametek, 2015.
[84] W. Liu, L. T. Drzal, A. K. Mohanty, and M. Misra, “Influence of processing methods and fiber length on physical properties of kenaf fiber reinforced soy based biocomposites,” *Compos. Part B Eng.*, vol. 38, no. 3, pp. 352–359, Apr. 2007.
[85] M. Pracella, D. Chionna, I. Anguillesi, Z. Kulinski, and E. Piorkowska, “Functionalization, compatibilization and properties of polypropylene composites with Hemp fibres,” *Compos. Sci. Technol.*, vol. 66, no. 13, pp. 2218–2230, Oct. 2006.
[86] C. Baley, “Analysis of the flax fibres tensile behaviour and analysis of the tensile stiffness increase,” *Compos. Part Appl. Sci. Manuf.*, vol. 33, no. 7, pp. 939–948, Jul. 2002.
[87] I. Jarvis and K. E. Jarvis, “Inductively coupled plasma-atomic emission spectrometry in exploration geochemistry,” *J. Geochem. Explor.*, vol. 44, no. 1, pp. 139–200, Jul. 1992.
[88] EAG Laboratories Incorporated, “ICP-OES and ICP-MS Detection Limit Guidance,” *EAG Laboratories*. [Online]. Available: https://www.eag.com/resources/appnotes/icp-oes-and-icp-ms-detection-limit-guidance/. [Accessed: 09-Aug-2018].
[89] Radboud University, “ICP-MS,” *General Instrumentation*. [Online]. Available: https://www.ru.nl/science/gi/facilities-activities/elemental-analysis/icp-ms/. [Accessed: 09-Aug-2018].
[90] “Ultra Centrifugal Mill ZM 200 - RETSCH.” [Online]. Available: https://www.retsch.com/products/milling/rotor-mills/zm-200/function-features/. [Accessed: 24-May-2018].
[91] ASTM International, “ASTM D638-14 Standard Test Method for Tensile Properties of Plastics.” 2014.
[92] J. Morgan and E. Connoly, “Plant-Soil Interactions: Nutrient Uptake,” *Nat. Educ.*, vol. 4, no. 8, 2013.
[93] Central Facility for Advanced Microscopy and Microanalysis, “Introduction to Energy Dispersive X-ray Spectrometry (EDS).” University of California, Riverside.

Appendix

Peak deconvolution code produced with help from Rasool Nasseri and Ward Madill. Attempts on peak deconvolution was done to separate cellulose and hemicellulose peaks to quantify their respective concentrations. Peak deconvolution would be successful if the fitted curve matched the actual cure in Figure 32.

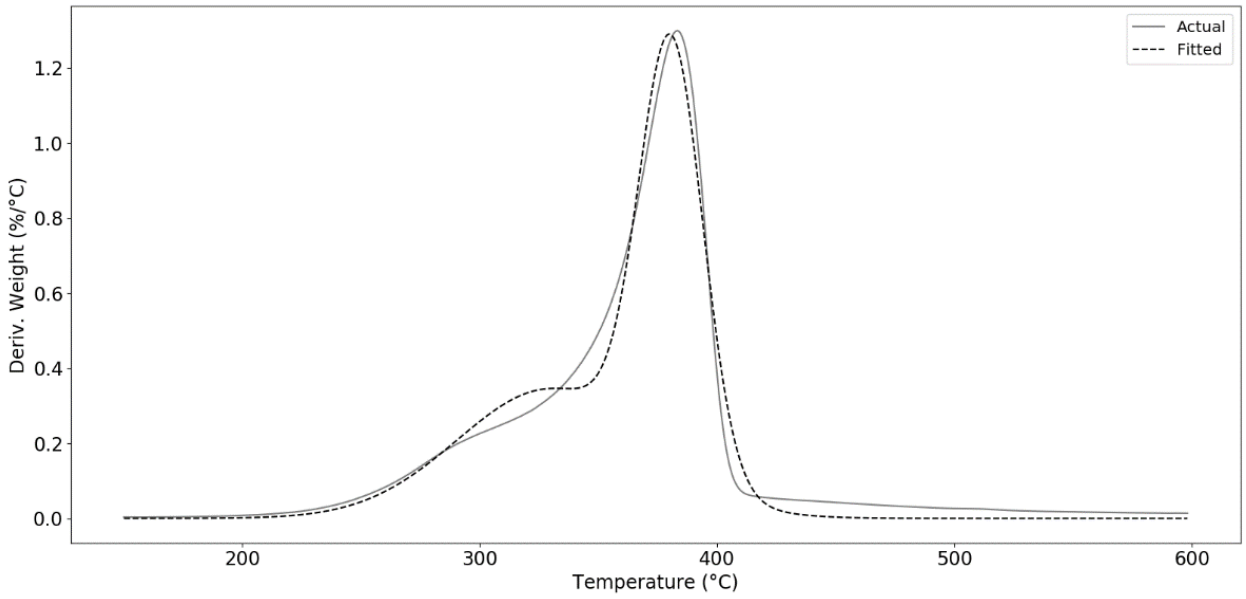

Figure 32: TGA peak deconvolution. Actual is experimental data of 0-RT MKF. Fitted is the curve from model fitting.

Associated Python code for peak deconvolution:

```
import pandas as pd
import numpy as np
import matplotlib.pyplot as plt
```

```
import scipy as sp
import lmfit

file1 = "/home/krishna/Documents/newfiles/0-RT.xlsx"
file2 = "/home/krishna/Documents/newfiles/0-80.xlsx"
file3 = "/home/krishna/Documents/newfiles/3-RT.xlsx"
file4 = "/home/krishna/Documents/newfiles/3-80.xlsx"
file5 = "/home/krishna/Documents/newfiles/6-RT.xlsx"
file6 = "/home/krishna/Documents/newfiles/6-80.xlsx"

df1 = pd.read_excel( file1, sheetname=0 )
df2 = pd.read_excel( file2, sheetname=0 )
df3 = pd.read_excel( file3, sheetname=0 )
df4 = pd.read_excel( file4, sheetname=0 )
df5 = pd.read_excel( file5, sheetname=0 )
df6 = pd.read_excel( file6, sheetname=0 )
dat= [df1, df2, df3, df4, df5, df6]


# In[3]:


Temp1 = np.array(df1['Temperature (°C)'].dropna().values)
Rate1 = np.array(df1['Deriv. Weight (%/°C)'].dropna().values)
Perc1 = np.array(df1['Mass Percentage (%)'].dropna().values)
Temp2 = np.array(df2['Temperature (°C)'].dropna().values)
Rate2 = np.array(df2['Deriv. Weight (%/°C)'].dropna().values)
Perc2 = np.array(df2['Mass Percentage (%)'].dropna().values)
Temp3 = np.array(df3['Temperature (°C)'].dropna().values)
Rate3 = np.array(df3['Deriv. Weight (%/°C)'].dropna().values)
Perc3 = np.array(df3['Mass Percentage (%)'].dropna().values)
Temp4 = np.array(df4['Temperature (°C)'].dropna().values)
Rate4 = np.array(df4['Deriv. Weight (%/°C)'].dropna().values)
Perc4 = np.array(df4['Mass Percentage (%)'].dropna().values)
Temp5 = np.array(df5['Temperature (°C)'].dropna().values)
Rate5 = np.array(df5['Deriv. Weight (%/°C)'].dropna().values)
Perc5 = np.array(df5['Mass Percentage (%)'].dropna().values)
Temp6 = np.array(df6['Temperature (°C)'].dropna().values)
Rate6 = np.array(df6['Deriv. Weight (%/°C)'].dropna().values)
Perc6 = np.array(df6['Mass Percentage (%)'].dropna().values)


from lmfit.models import (GaussianModel, SkewedGaussianModel,
MoffatModel, VoigtModel, PseudoVoigtModel,
LorentzianModel, DonaichModel, ExponentialGaussianModel)
```

```
Hemi=GaussianModel(prefix='Hemi_')
Cell=GaussianModel(prefix='Cell_')
Lig=LorentzianModel(prefix='Lig_')
pars = Hemi.guess(Rate1[np.where(Temp1>150)],
x=Temp1[np.where(Temp1>150)], center=290)
pars += Cell.guess(Rate1[np.where(Temp1>150)],
x=Temp1[np.where(Temp1>150)], center=370)
pars['Hemi_center'].set(min=200, max=330)
pars['Hemi_height'].set(min=0)
mod = Hemi + Cell
out = mod.fit(Rate1[np.where(Temp1>150)], pars,
x=Temp1[np.where(Temp1>150)])


print(out.fit_report())
plt.figure(3)
plt.plot(Temp1[np.where(Temp1>150)], Rate1[np.where(Temp1>150)],
'r', label = 'Actual')
plt.plot(Temp1[np.where(Temp1>150)], out.best_fit, 'k--', label
='Fitted')
plt.xlabel('Temperature (°C)')
plt.ylabel('Deriv. Weight (%/°C)')
plt.legend()
plt.show()
```